Drug-target residence time : a case for the adenosine A1 and A2A receptors

Guo, D.

Chapter 4

Binding kinetics of ZM241385 derivatives at the human adenosine A_{2A} receptor

Guo D, Xia L, Van Veldhoven JPD, Hazeu M, Mocking T, Brussee J,
IJzerman AP, Heitman LH.
Adapted from: *ChemMedChem,* 2014; 9(4): 752-761

About this chapter

Classical drug design and development rely mostly on affinity- or potency-driven structure-activity relationships (SAR). So far a compound's binding kinetics has been largely ignored, which importance, however, is now increasingly recognized. In this chapter we performed an extensive structure-kinetics relationship (SKR) study in addition to a traditional SAR analysis at the adenosine A_{2A} receptor ($A_{2A}R$). The ensemble of 24 $A_{2A}R$ compounds, all triazolotriazine derivatives resembling the prototypic antagonist ZM241385 (4-(2-((7-amino-2-(furan-2-yl)-[1,2,4]triazolo[1,5-*a*][1,3,5]triazin-5-yl) amino)ethyl)phenol), displayed only minor differences in affinity, while they varied substantially in their dissociation rates from the receptor. We believe that such a combination of SKR and SAR analysis as on the $A_{2A}R$ will have general importance for the superfamily of G protein-coupled receptors, since it can serve as a new strategy to tailor the interaction between ligand and receptor.

4.1 Introduction

G protein-coupled receptors (GPCRs) are among the largest and most heavily investigated drug targets in the drug research community. Traditional early phase drug design and discovery campaigns of GPCRs largely depend on equilibrium affinity- or potency-based structure-activity relationships (SAR). This approach of lead optimization allows a quick synthesis-evaluation feedback loop to pool abundant candidate compound assemblies for further drug evaluation. Nevertheless, this classical SAR approach does not seem to predict clinical efficacy very well, which is witnessed by the high levels of attrition during the translation of a lead's *in vitro* activity into its *in vivo* and clinical evaluation. To address this issue, several recent reviews have emphasized the importance of binding kinetics, and in particular the life time of a drug-target binary complex, i.e., drug-target residence time (RT), as a critical differentiator and predictor for drug efficacy and safety.[1-5] Next to the RT, the association rate of a ligand-receptor interaction, which reflects the 'target-engagement time' (ET), should also be taken into consideration in the early phases of drug research. This is especially important for designing drugs that require a fast on-set of action and potentially for drugs that act on temporarily existing targets, such as protein-protein interactions.[6-11] Therefore, an extensive structure-kinetics relationship (SKR) investigation, in addition to the traditional SAR analysis, can be of great use in the early phases of candidate drug optimization.

The human adenosine A_{2A} receptor ($A_{2A}R$) is a subtype of adenosine receptors (others are A_1, A_{2B} and A_3), belonging to the superfamily of GPCRs.[12] Antagonists for this receptor have been reported as potential treatment for Parkinson's disease.[13] As such, many compounds with high $A_{2A}R$ affinities have been developed,[14-16] including the reference antagonist ZM241385 (4-(2-((7-amino-2-(furan-2-yl)-[1,2,4]triazolo[1,5-*a*][1,3,5]triazin-5-yl) amino)ethyl)phenol)—a triazolotriazine derivative (Figure 4.1).[17,18] These compounds were well characterized and optimized in terms of their binding affinity and thus benchmarked for later medicinal chemistry attempts at the $A_{2A}R$. For example, Vu and colleagues synthesized ZM241385 derivatives with increased bioavailability.[19-21] However, the success rate of the developed $A_{2A}R$ antagonist in clinical trials is disappointingly low. This indicates the results of currently used pre-clinical animal models don't translate well into clinical studies. Moreover, little is known about their binding kinetics so far.

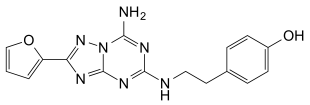

ZM241385

Figure 4.1 | Chemical structure of ZM241385.

Thus, we decided to further extend this series of compounds by progressively modifying them at the C_2 position, which would generate an insight into both SKR and SAR. We believe that the present study adds knowledge to our current understanding of drug design and development for $A_{2A}R$ antagonists. Hopefully, this methodology of combining both SKR and SAR can be generally applied at other drug targets as well in the future.

4.2 Results and discussion

Chemical synthesis

Synthesis routes are depicted in Scheme 4.1 and Scheme 4.2. In total, an ensemble of 24 triazolotriazine derivatives (**12a-x**) was obtained. Notably, compounds **12a**, **12b** and **12x** were previously reported by Vu *et al.*,[21] and resynthesized in the present chapter, although in a different synthetic approach. All compounds (**12a-x**) started from furan-2-carbohydrazide (**1**) to generate 7-amino-2-(furyl)-5-methylthio[1,2,4]triazolo[1,5-*a*][1,3,5] triazine (**4**), following the synthetic approach reported by Dolzhenko *et al.* and Jörg *et al.*[22-25] Subsequently, **4** was oxidized with 3-chloroperbenzoic acid (MCPBA) to afford the corresponding sulfoxide/sulfone mixture **5**,[26] which was substituted with a variety of commercially available amines (**11f-h**) to generate **12f-h** or with in-house prepared amines (**11a-d** and **11i-x**) to generate **12a-d** and **12i-x**. **12e** was obtained by the *N*-Boc deprotection of **12d**.

For the preparation of intermediate amines **11a-d** and **11i-x**, synthetic routes are depicted in Scheme 4.2. In brief, reactions were carried out via *N*-alkylation of the commercially available piperazine derivatives (**9a-d** and **9i-u**) or the in-house synthesized phenylpiperazines (**9v-x**), which were

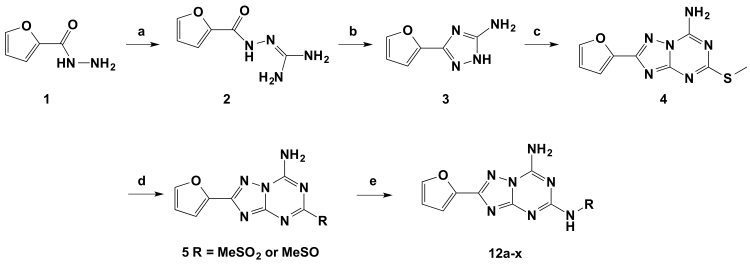

Scheme 4.1 | General synthesis route to 24 triazolotriazine derivatives. *Reagents and conditions*: (a) S-methylisothiourea sulfate (2:1), 4 % $NaOH_{(aq)}$ RT; (b) H_2O, RT; (c) (1) $(MeS)_2C{=}NCN$, heat, 180 ˚C, (2) CH_2Cl_2-CH_3OH (2:1), reflux; (d) *m*CPBA (70 % strength), CH_2Cl_2, 0 ˚C-> RT; (e) $(Et)_3N$, CH_3CN.

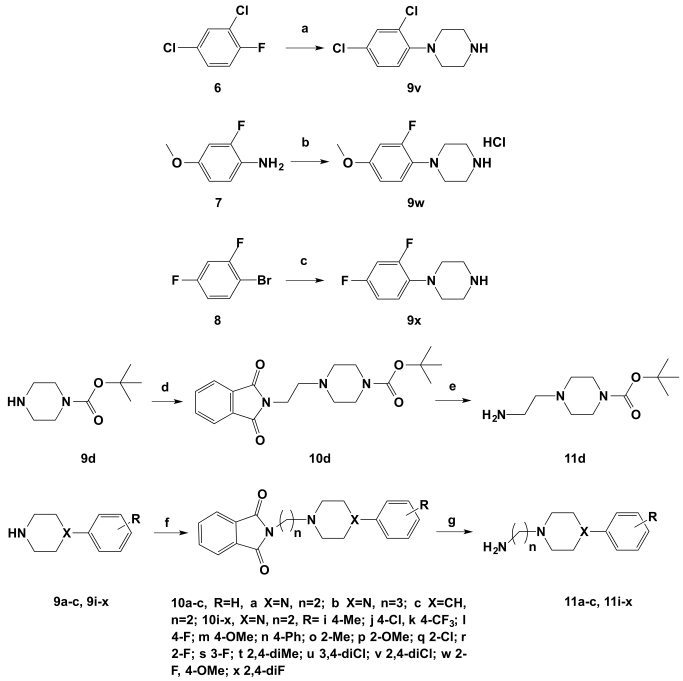

Scheme 4.2 | Preparation of key intermediates. *Reagents and conditions*: (a) piperazine, *N,N*-dimethylacetamide, 165 ˚C; (b) bis(2-chloroethyl)amine hydrochloride, Na_2CO_3, 130 ˚C, butanol; (c) *t*-BuONa, BINAP, $Pd_2(dba)_3$, toluene, N_2, 110 ˚C; (d) K_2CO_3, NaI, butanone, reflux; (e) H_2NNH_2-H_2O, EtOH; (f) 3-bromo-alkylphthamide, K_2CO_3, DMF, 70 ˚C; (g) H_2NNH_2-H_2O, EtOH, 70 ˚C.

derived from **6-8**, **27-30** to obtain the appropriate *N*-phthalimide-protected alkyl piperazines (**10a-d** and **10i-x**). This was followed by deprotection of the phthalimide to afford the free amines (**11a-d** and **11i-x**).

SAR and SKR of triazolotriazine derivatives

The SAR and SKR analyses were initiated by testing two compounds, **12a** and **12b**, and then chemical modifications were gradually introduced to these two compounds (Table 4.1). Several observations were made; (1) the molecule with a two-carbon spacer was superior to the compound with a three-carbon spacer. The former (**12a,** K_i = 0.30 ± 0.08 nM; RT = 164 ± 32 min) displayed a four-fold higher affinity and 41-fold longer RT than the latter (**12b**, K_i = 1.3 ± 0.1 nM; RT = 4 ± 1 min). Such a variation of the linker length also resulted in different association rates (**12a**, k_{on} = 0.051 ± 0.005 $nM^{-1}{\cdot}min^{-1}$; **12b**, k_{on} = 0.16 ± 0.06 $nM^{-1}{\cdot}min^{-1}$). (2) Upon different degrees of C_2-phenylpiperazine modification the ligands' affinities were moderately to largely affected, while their receptor RTs were drastically shortened (**12d-h**), except for the Boc-protected intermediate **12d**. This compound, in fact, had a 30-fold and 20-fold improved affinity and RT, respectively, in comparison to its truncated analogue (**12e**). Moreover, their ETs were also significantly influenced by the chemical modifications on the phenylpiperazine moiety. Specifically, **12g** displayed the fastest association rate of 0.046 ± 0.020 $nM^{-1}{\cdot}min^{-1}$. (3) Receptor RTs of **12a** or **12d** highlight the preference of an electron-withdrawing effect at the piperazine amine moiety. The insertion of an additional carbon into **12a** (between the piperazine and the phenyl group; **12g**) reversed the electron-withdrawing effect into a donating effect, which resulted in a reduced $A_{2A}R$ affinity (8.1 ± 0.5 nM) and RT (4 ± 1 min). Replacement of the nitrogen by a carbon atom on the 'right side' of the piperazine (compare **12a** and **12c**) resulted in strongly decreased RT values that further confirmed the nitrogen's importance in maintaining $A_{2A}R$ affinity and RT (Table 4.1, Figure 4.2 for **12c**). Notably, ET and RT of **12c** were the shortest of this series of compounds (except for the nearly 20-fold lower affinity compound **12h**) without a large compromise on its affinity. Taken together, these results highlight the importance of the C_2-phenylpiperazine-ethyl group, and more specifically show that the electron-deficient nitrogen (on the right side of the piperazine) has a role in preserving a tight and enduring ligand-receptor interaction.

Table 4.1 | Binding affinities and kinetics of ZM241385 and 12a-12h.

	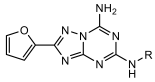	$hA_{2A}R$				hA_1R
Compd	Structure, R=	K_i (nM)[a]	k_{on} ($nM^{-1}\cdot min^{-1}$)[b]	k_{off} (min^{-1})[b]	RT (min)[c]	K_i (nM) or %[d]
ZM241385	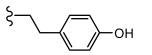	0.40 ± 0.03	0.13 ± 0.06	0.014 ± 0.003	71 ± 21	255[23]
12a	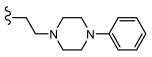	0.30 ± 0.08	0.051 ± 0.005	0.0061 ± 0.0020	164 ± 32	8%
12b	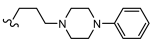	1.3 ± 0.1	0.16 ± 0.06	0.25 ± 0.01	4 ± 1	30%
12c	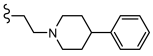	3.8 ± 0.8	0.20 ± 0.1	0.35 ± 0.03	3 ± 1	22%
12d	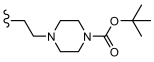	1.5 ± 0.1	0.030 ± 0.003	0.012 ± 0.004	83 ± 17	2%
12e	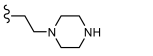	45 ± 0.1	0.0063 ± 0.0030	0.24 ± 0.10	4 ± 1	10%
12f	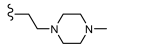	31 ± 6	0.0057 ± 0.0020	0.25 ± 0.10	4 ± 1	11%
12g	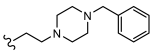	8.1 ± 0.5	0.046 ± 0.020	0.24 ± 0.10	4 ± 1	21%
12h	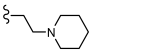	64 ± 1	0.020 ± 0.002	0.62 ± 0.08	2 ± 0	32%

[a] Displacement of specific [^{3}H]-ZM241385 binding from the $hA_{2A}R$ at 4 ˚C. [b] k_{on} and k_{off} were determined in competition association assay at 4 ˚C. [c] RT (Residence Time) = 1 / k_{off}. [d] % displacement of specific [^{3}H]-DPCPX binding at 1 μM from the hA_1R at 25 ˚C. Data are shown as mean ± s.e.m of three separate experiments each performed in duplicate.

SAR and SKR were further analyzed with 16 phenyl-substituted **12a** analogues (Table 4.2, **12i-x**). Upon *para*-substitution at the phenyl ring (**12i-n**), no significant change of the ligands' affinity (K_i values < 1 nM) was observed, except for **12n** which had a 4.7-fold decrease in affinity (1.4 ± 0.2 nM). The latter was probably caused by steric hindrance induced by the bulky phenyl substituent, which presumably also limited its RT to 29 ± 2 min and decreased the association rate to 0.018 ± 0.002 $nM^{-1}\cdot min^{-1}$. In contrast, the other *para*-substituted compounds **12i-m** displayed a similar duration of *in vitro* receptor occupancy as ZM241385 (RT = 71 ± 21 min). In comparison to the convergent results upon *para*-position modifications,

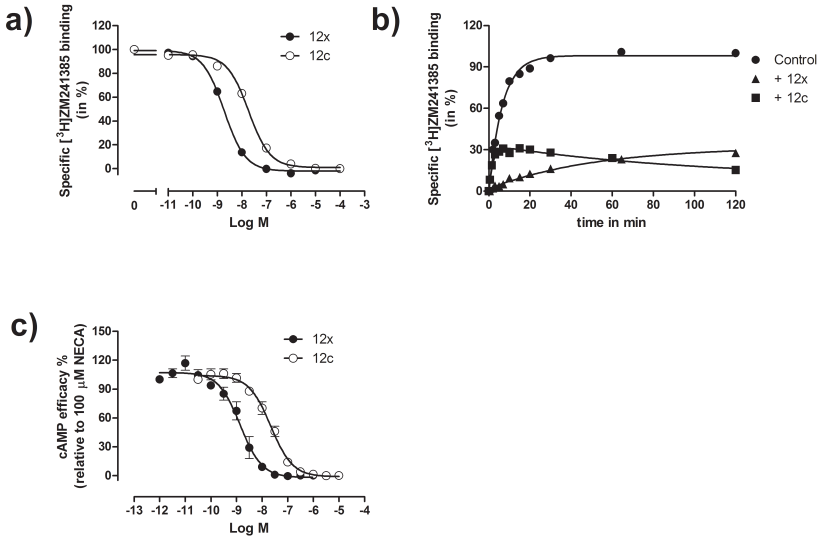

Figure 4.2 | (a) Displacement of specific [^{3}H]-ZM241385 binding from the hA_{2A} receptor by two representative compounds, namely **12x** and **12c**; (b) [^{3}H]-ZM241385 competition association binding in the absence of ligand (control) and in the presence of 10 × K_i of unlabeled **12x** or **12c**. Data was fitted to the equation described in the experimental section to calculate k_{on} and k_{off} of unlabeled ligands. Representative graphs from one experiment performed in duplicate (See Table 4.1 and 4.2 for affinity and kinetic values); (c) Concentration-effect curves for **12x** and **12c** in a cAMP assay. Data were obtained by adding HEK293hA_{2A}R cells to the mixture of the antagonist (**12x** or **12c**) and 100 nM NECA for an incubation of 30 min. Data are expressed as mean ± s.e.m from at least three independent experiments. (See Table 4.3 for potency values).

ortho-substituted analogues (**12o**-**12r**) displayed divergent affinities and binding kinetics. Specifically, an *ortho*-methoxy substituent (**12p**) decreased A_{2A}R affinity and RT compared to its *para*-substituted analogue (**12m**), while the methyl- (**12o**) or halogen-substituted (**12q**, **12r**) analogues displayed increased A_{2A}R affinities and RTs. For most compounds disubstitution of the phenylpiperazine did not dramatically change their affinities or binding kinetics (**12t-w**). Interestingly for **12x**, bearing an *ortho*- and *para*-fluoro substituent, an exceptionally long receptor RT of 323 ± 25 min was found (Table 4.2) that was much longer than the simple 'sum RT' of mono-fluorinated analogues (**12l**, **12r** and **12s**) and almost five-fold longer than

Table 4.2 | Binding affinities and kinetics of 12i-12x.

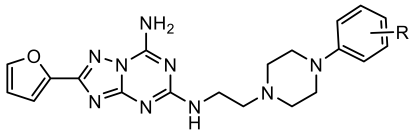

Compd	R=	$hA_{2A}R$				hA_1R
		K_i (nM) [a]	k_{on} ($nM^{-1}\cdot min^{-1}$) [b]	k_{off} (min^{-1}) [b]	RT (min) [c]	K_i (nM) or % [d]
12i	4-CH_3	0.79 ± 0.06	0.062 ± 0.020	0.016 ± 0.006	63 ± 18	14 %
12j	4-Cl	0.29 ± 0.10	0.090 ± 0.010	0.018 ± 0.006	56 ± 11	35 ± 13
12k	4-CF_3	0.38 ± 0.10	0.072 ± 0.009	0.020 ± 0.005	50 ± 37	64 %
12l	4-F	0.54 ± 0.05	0.10 ± 0.02	0.020 ± 0.005	50 ± 8	57 %
12m	4-OCH_3	0.51 ± 0.10	0.064 ± 0.005	0.0079 ± 0.0020	127 ± 19	11 %
12n	4-Ph	1.4 ± 0.2	0.018 ± 0.002	0.034 ± 0.010	29 ± 2	32 %
12o	2-CH_3	0.13 ± 0.04	0.062 ± 0.002	0.0075 ± 0.0020	133 ± 21	29 %
12p	2-OCH_3	3.5 ± 0.7	0.032 ± 0.003	0.070 ± 0.070	14 ± 11	19 %
12q	2-Cl	0.13 ± 0.03	0.068 ± 0.016	0.0065 ± 0.0010	154 ± 25	30 %
12r	2-F	0.12 ± 0.05	0.052 ± 0.012	0.011 ± 0.002	91 ± 15	28 %
12s	3-F	0.29 ± 0.03	0.055 ± 0.009	0.012 ± 0.003	83 ± 14	62 %
12t	2, 4-diCH_3	0.16 ± 0.01	0.11 ± 0.02	0.012 ± 0.001	78 ± 9	29 %
12u	3, 4-diCl	0.31 ± 0.10	0.10 ± 0.01	0.015 ± 0.004	67 ± 11	21 ± 4
12v	2, 4-diCl	0.15 ± 0.02	0.11 ± 0.01	0.014 ± 0.001	70 ± 5	80 ± 24
12w	2-F, 4-OCH_3	0.24 ± 0.05	0.054 ± 0.005	0.0083 ± 0.0010	120 ± 65	27%
12x	2, 4-diF	0.33 ± 0.04	0.034 ± 0.004	0.0031 ± 0.0002	323 ± 25	22%

[a] Displacement of specific [^{3}H]-ZM241385 binding from the $hA_{2A}R$ at 4 ˚C. [b] k_{on} and k_{off} were determined in competition association assay at 4 ˚C. [c] RT (Residence Time) = 1 / k_{off}. [d] % displacement of specific [^{3}H]-DPCPX binding at 1 μM from the hA_1R at 25 ˚C. Data are shown as mean ± s.e.m of three separate experiments each performed in duplicate.

ZM241385's RT. From Figure 4.2B it also follows that **12x** had a much longer RT than ZM241385 (the radioligand), since a typical 'overshoot' in specific radioligand binding was observed.[30] On the contrary, if a competitor dissociates faster from its target than the radioligand, the specific binding of the radioligand will slowly and monotonically approach its equilibrium over time, as observed for **12c** (Figure 4.2B).[30]

Almost all prepared ZM241385 derivatives displayed high selectivity over the human adenosine A_1 receptor (A_1R), i.e., < 50 % of [^{3}H]-DPCPX displacement at 1 μM (Table 4.1 and 4.2). Notably, the longest RT compound on the $A_{2A}R$, **12x**, had a very good $A_{2A}R$ selectivity over the A_1R (Table 4.2). In contrast, **12j**, **12u** and **12v**, with mono- or di-chloro substitution, lost some selectivity over the A_1R (K_i values at the A_1R ranged from 20 nM to 80 nM, Table 4.2). Interestingly, all these compounds contain a chloro-substituent in the *para*-position, yet the substituent in other positions (e.g., **12q**, *ortho*-substituent) didn't exhibit lower selectivity for the $A_{2A}R$ over the A_1R.

Functional characterization of **12x** and **12c** in a cAMP assay

Subsequently, the longest and shortest RT compounds with high affinity (i.e., **12x** and **12c**) were functionally characterized in an $A_{2A}R$ agonist-induced cAMP assay, which revealed their antagonistic behavior. Firstly, it follows from Figure 4.2C that both **12x** and **12c** induced a concentration-dependent decrease of intracellular cAMP levels with 16-fold difference in their IC_{50} values, which are 1.4 ± 0.1 nM and 21.8 ± 0.5 nM, respectively (Table 4.3). Secondly, pre-treatment of HEK293h$A_{2A}R$ cells with different concentrations of **12x** before stimulation with an AR agonist (i.e., 5'-*N*-ethylcarboxamidoadenosine, NECA) induced insurmountable antagonism. In other words, the NECA concentration-effect curve was shifted to the right with a concomitant decrease in the maximal response (Figure 4.3A). Conversely, **12c** displayed surmountable $A_{2A}R$ antagonism, shifting NECA's curves to the right yet without affecting its maximal response (Figure 4.3B). In addition, the pA_2 value for **12c** generated from a Schild-plot was 8.62 ± 0.29, which was similar to its pK_i value (8.40 ± 0.10), and the Schild-slope was close to unity (0.93 ± 0.11) suggesting that **12c** competed with NECA for the same receptor binding site. To further examine whether **12x** and **12c** both bound to the same site as the agonist, we also

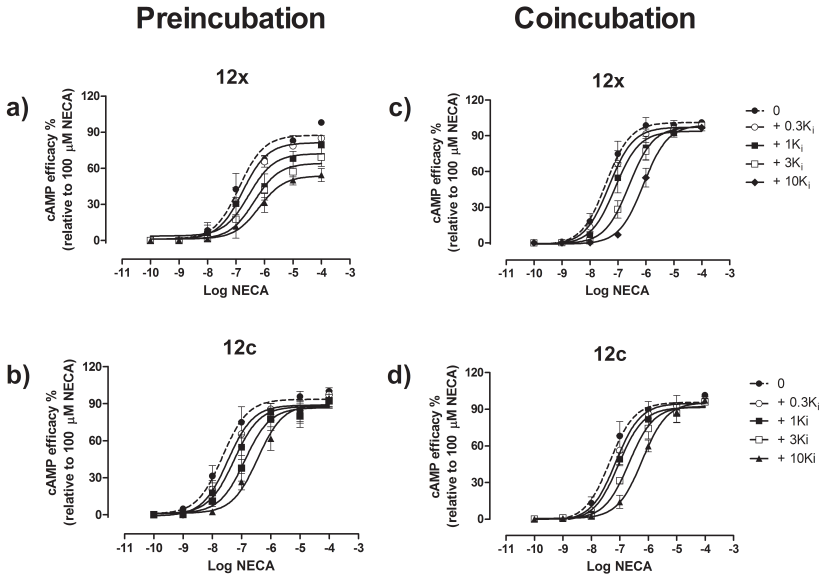

Figure 4.3 | cAMP experiments were performed on human embryonic kidney 293 cells stably expressing the $hA_{2A}R$ at ambient room temperature (22–25 °C). 12x (a) or **12c** (b) were incubated for 30 min prior to the challenge of the adenosine receptor agonist NECA at a concentration ranging from 100 µM to 0.1 nM for another 30 min. **12x** (c) or **12c** (d) were co-incubated with NECA, at a concentration ranging from 100 µM to 0.1 nM, for 30 min. The agonist curves were generated in the presence of increasing concentrations of antagonist, namely 0.3-, 1-, 3- and 10-fold their respective K_i values. Data were normalized according to the maximal response produced by 100 µM NECA. The shift in agonist EC_{50} was determined to perform Schild analyses. Data are expressed as mean ± s.e.m from at least three independent experiments performed in duplicate.

performed a co-incubation experiment with **12x** or **12c** in the presence of NECA. It follows from Figure 4.3C and 4.3D that in this experimental set-up both compounds produced a rightward shift in the NECA dose-response curve without a suppression of the maximal response, i.e., indicative of a competitive interaction. Hence, these findings oppose that insurmountable antagonism resulted from an allosteric mode of inhibition, which would be proven by a suppression of the maximal response in the co-incubation experiment.[31-33] Notably, the generated pA_2 values of **12x** and **12c** in this experimental set-up were similar to their pK_i values and the derived Schild

Table 4.3 | Functional characterization of 12x and 12c in a cAMP assay.

	Potency [a]	Pre-incubation [b]		Co-incubation [b]	
Compd	IC_{50} (nM)	pA_2	Schild slope	pA_2	Schild slope
12c	1.4 ± 0.1	8.62 ± 0.29	0.93 ± 0.11	8.57 ± 0.06	0.93 ± 0.02
12x	21.8 ± 0.5	*N.A*	*N.A*	9.69 ± 0.03	1.13 ± 0.01

[a] Antagonists' potency (IC_{50}) values were determined from concentration-response curves for **12x** and **12c** in the presence of 100 nM NECA for a co-incubation of 30 min. Antagonists were pre-incubated for 30 min [b] or co-incubated [c] with NECA at a concentration ranging from 100 μM to 0.1 nM. *N.A.*, not applicable. Data are shown as mean ± s.e.m of three separate experiments each performed in duplicate at room temperature (22–25 °C).

slopes were close to unity (Table 4.3). Together, this confirmed that **12x** or **12c** bound fully competitively with NECA and the insurmountable $A_{2A}R$ antagonism of **12x** was a result caused by so-called hemi-equilibrium during the functional assay due to its long $A_{2A}R$ residence time profile.[32]

It needs to point out that the results for functional characterization and binding kinetics determination are not obtained at a physiologically more relevant temperature (37 ˚C) and thus cannot be representative for residence times observed *in vivo*. However, it is reasonable to expect that the ranking of these compounds' RTs at 4 ˚C should agree with the result at the room temperature or at the physiologically more relevant 37 ˚C. Such a discussion has been documented in our previous publication at the $A_{2A}R$, where UK432,097 has a RT five-fold the length of CGS21680.[34,35] This difference at 4 ˚C well translates into distinct duration of action in an *in vivo* setting reported by Mantell *et al.*, that is, 8 h for UK432,097 and less than one hour for CGS21680.[36]

Generation of a 'kinetics map' and physicochemical correlation plots from $A_{2A}R$ antagonist SKR data

Next, we plotted an on-/off-rate graph or so-called 'kinetics map', including the data of all $A_{2A}R$ ligands obtained in this chapter (Figure 4.4).[37] Evidently, this kinetics map depicted the ligand-receptor binding affinity (K_D, represented by the parallel diagonal lines) into detailed kinetic rates that reflect the process of 'target-engagement time' (k_{on}, Y axis) and the target-residence time (k_{off}, X

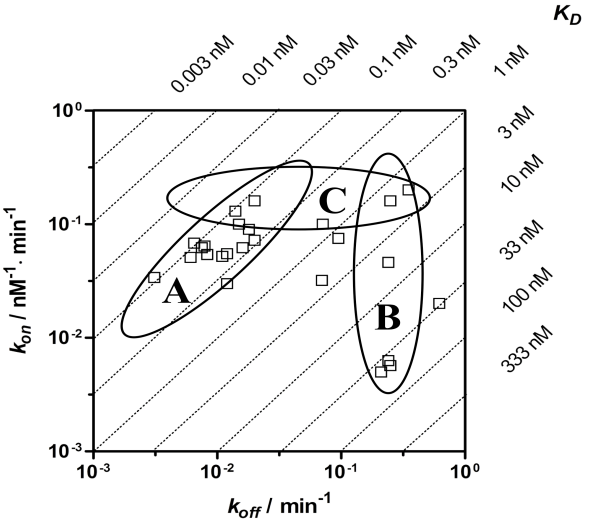

Figure 4.4 | The kinetics map (Y axis: k_{on}, $nM^{-1}{\cdot}min^{-1}$; X axis: k_{off}, min^{-1}) of all $A_{2A}R$ ligands that were tested in this chapter. The kinetically derived affinity ($K_D = k_{off} / k_{on}$) is represented by the parallel diagonal lines. Group A: compounds that have varied k_{on} and k_{off} values, while the K_D remained within a similar range (0.1-0.3 nM). Group B: compounds that have the same k_{off} values, but divergent K_D values. Group C: compounds that have the same k_{on} values, but divergent K_D values.

axis), respectively. We observed that the compounds can be divided into three groups; firstly, both k_{on} and k_{off} values can vary across one order of magnitude (Figure 4.4, Group A), while the K_D remained within a narrow range (0.1-0.3 nM), as mentioned above. This indicated that compounds with the same affinity may have many different combinations of on- and off-rates even within the same scaffold and target system. Such information, often ignored or unavailable in traditional SAR studies, in fact can be highly decisive in translating a lead's *in vitro* profile into *in vivo* pharmacokinetics (PK) and/or pharmacodynamics (PD) behavior.[38] Secondly, compounds sharing the same off-rate may bear divergent K_D values, due to different on-rates (Group B). It has been shown in several cases that a compound's slow dissociation rate was pivotal for a high *in vivo* efficacy.[34,35] Thus, in retrospect one could imagine that many compounds with promising k_{off} values were overlooked simply due to their 'low scores' in classical affinity- or potency-dominated evaluations.

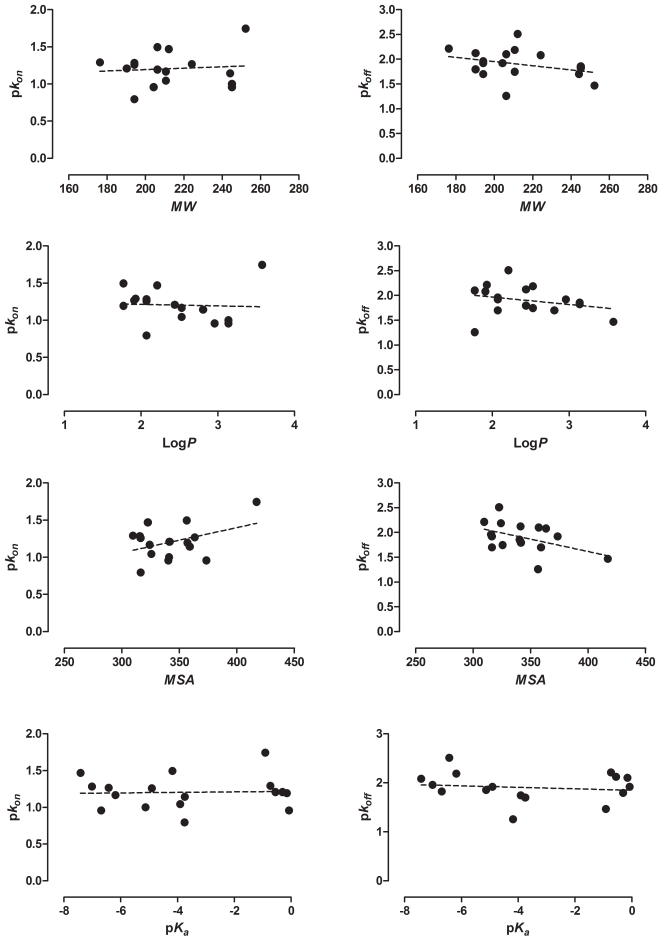

Figure 4.5 | Molecular descriptors of size (MW), lipophilicity (logP), molecular surface area (MSA, 3D), and charge (pK_a) of the substituted C_2-phenylpiperazine fragments and their correlation with the –log values of on- and off-rates. No obvious linear correlation was observed between the association-/dissociation-rates and MW (for association: r^2 = 0.0089, P = 0.7180; for dissociation: r^2 = 0.1059, P = 0.2024), logP (for association: r^2 = 0.0023, P = 0.8563; for dissociation: r^2 = 0.0731, P = 0.2938), MSA (for association: r^2 = 0.1629, P = 0.1082; for dissociation: r^2 = 0.2107, P = 0.0638) or pK_a (for association: r^2 = 0.0018, P = 0.8727; for dissociation: r^2 = 0.0187, P = 0.6010).

Thirdly, the same holds for a compound's on-rate (Group C), i.e., merely focusing on a ligand's K_D can result in compounds without the desired on-rate, as exemplified by candidate drugs aiming at acute diseases where a rapid on-set of action is desired (e.g., acute respiratory distress syndrome).[6,11] Taken together, the kinetics map provides a detailed interpretation of a ligand-receptor binding process with a full inventory of k_{on}, k_{off} and K_D values of a series of compounds.

Furthermore, molecular and physicochemical properties of the synthesized phenylpiperazine analogues (**12i-x** and **12a**) and their putative relationship with the on- and off-rates were examined in efforts to identify key factor(s) affecting their binding kinetics (Figure 4.5). Since the main scaffold of these series of compounds is the same, we specifically focused on the properties of C_2-phenylpiperazine fragments. Several descriptors were selected to be further examined in correlation plots. They were the size (molecular weight, MW), surface of the fragment (molecular surface area, MSA), lipophilicity (logP), and charge (ionization constant, pK_a). There was no obvious linear correlation between the association-/dissociation-rates and MW, logP, MSA or pK_a. We also performed a multiple linear regression analysis to check whether the compound's binding kinetics is directed by a combination of two or more of the physicochemical descriptors. However, no significant correlation was found either (significance $F > 0.05$ in all cases). Altogether, this indicated that the binding kinetics was compound specific and that there is no general trend in the correlation to their molecular and physicochemical properties.

Importance of the phenylpiperazine-fragment at the C_2 position and its location in the $A_{2A}R$'s 'vestibule'

In this chapter we observed that upon minor chemical modifications of the phenylpiperazine side chain on the triazolotriazine scaffold (Table 4.1 and 4.2), binding affinity of the derivatives underwent subtle changes only, while their binding kinetics were very sensitive to such structural variations. For instance, upon substitution of **12a**, **12k** (*para*-trifluoromethyl substituted) displayed a similar K_i value as **12a**, while its off-rate was 3.4-fold increased. In another case, the on- and off-rates of **12u** (*meta*-, *para*-chloro disubstituted) were increased and decreased, respectively, in a similar magnitude (approximately

2-fold), hence leading to an unchanged affinity value compared to **12a**. Table 4.2 as a whole exemplifies the difficulty of selecting a 'next-stage' candidate based on SAR alone. Most compounds have subnanomolar affinity, and compound **12x** does not stand out in any particular way.

The lack of large changes in binding affinities might be expected given the absence of direct interactions between the phenylhydroxyl group and the receptor in a recently determined high-resolution crystal structure of ZM241385-bound $A_{2A}R$.[39] In this structure, the phenylhydroxyl group points away from the binding pocket toward the extracellular space. Likewise, in another crystal structure of UK432,097-bound $A_{2A}R$, the bulky tail of the agonist UK432,097 at the adenine C_2 position extends outward of the ligand-binding cavity.[40] Notably, it was recently published that this agonist also has a slow association rate and long RT at the $A_{2A}R$.[34] Based on these findings, we postulated that the C_2-phenylpiperazine group protrudes outward without forming direct interactions with residues in the binding pocket of the triazolotriazine core. Instead, it may interact with residues that are located at the extracellular loops or the adjacent regions topping the binding cavity, on its trajectory of associating to or dissociating from the receptor. Such reasoning is supported by a recent molecular dynamics simulation study of the β_1- and β_2-adrenergic receptors by Dror *et al.*[41] They found that several beta blockers and one beta agonist all traverse the same well-defined, dominant pathway as they bind to the β_1- and β_2-adrenergic receptors, initially making contact with a so-called 'vestibule' on the receptor's extracellular surface. Interestingly, this holds true for the ligand binding dynamics of the M_3 muscarinic acetylcholine receptor too. Simulation results indicated that as tiotropium binds to or dissociates from the receptor, it 'pauses' at an alternative binding site in the extracellular 'vestibule'.[42] Taken together, such an extracellular 'vestibule' appears to play an important role in the on- or off-trajectory to and from the binding pocket of a GPCR.[41] These molecular dynamics calculations therefore support that an extracellular 'vestibule' appears to play an important role in the on- or off trajectory to and from the binding pocket of a GPCR, which is in accordance with our observation that a change in the C_2-phenylpiperazine group significantly affected the ligand's association and dissociation rates at the $A_{2A}R$, while their K_i values were minimally changed.

4.3 Conclusion

We have exemplified an extensive structure-kinetics relationship (SKR) in addition to a traditional SAR analysis at the adenosine A_{2A} receptor ($A_{2A}R$). Compound **12x**, the high-affinity $A_{2A}R$ ligand previously reported by Vu *et al.*,[21] was revealed to have an exceptional long RT (323 min). Compared to the traditional SAR analysis, such a kinetic insight provided a further rationale to support the selection of **12x** from otherwise chemically and biologically similar compounds for further testing. Kinetics mapping all tested $A_{2A}R$ ligands also provided a detailed interpretation of the ligand-receptor binding process. Next, a functional comparison between a short RT antagonist **12c** and **12x** in the pre-incubation experiment further revealed **12x**'s insurmountable antagonism at the $hA_{2A}R$—a phenomenon distinct from **12c**. In addition, investigation of the molecular properties indicated that the ligand-receptor binding kinetics were most likely driven by specific interactions between the ligand and the receptor. It could also be of great interest to subject the compounds having similar affinity yet different binding kinetics into (pre) clinical tests, especially to examine how relevant the variation in RT and on/off-rate is in terms of *in vivo* efficacy and duration of action. We believe that SKR, in combination with traditional SAR, can serve as an important tool for more directed medicinal chemistry efforts in the future.

4.4 Experimental section

Chemical synthesis

General: All solvents and reagents were purchased from commercial sources and were of analytical grade. Demineralised water is simply referred to as H_2O, as it was used in all cases unless stated otherwise (i.e., brine). ^{1}H and ^{13}C NMR spectra were recorded on a Bruker AV 400 liquid spectrometer (^{1}H NMR, 400 MHz; ^{13}C NMR, 101 MHz) at ambient temperature. Chemical shifts are reported in parts per million (ppm), are designated by δ and are downfield to the internal standard tetramethylsilane (TMS). Coupling-constants are reported in Hz and are designated as *J*. High resolution mass

spectrometry was performed by the Leiden Institute of Chemistry and recorded by direct injection (2 µL of a 2 µM solution in water/MeCN; 50/50; v/v and 0.1 % formic acid) on a mass spectrometer (Thermo Finnigan LTQ Orbitrap) equipped with an electrospray ion source in positive mode (source voltage 3.5 kV, sheath gas flow 10, capillary temperature 275 °C) with resolution R = 60000 at *m/z* 400 (mass range *m/z* = 150-2000) and calibrated for dioctylphthalate (*m/z* = 391.28428). Analytical purity of the final compounds was determined by high performance liquid chromatography (HPLC) with a Phenominex Gemini 3u C18 110A column (50 x 4.6 mm, 3 µm), measuring UV absorbance at 254 nm. Sample preparation and HPLC method were as follows, unless stated otherwise: 0.3-0.8 mg of compound was dissolved in 1 mL of a 1:1:1 mixture of $CH_3CN/H_2O/t$-BuOH and eluted from the column within 15 minutes, with a three component system of H_2O/CH_3CN/1 % TFA in H_2O, decreasing polarity of the solvent mixture in time from 80/10/10 to 90/0/10. All compounds showed a single peak at the designated retention time and are at least 95 % pure. Thin-layer chromatography (TLC) was routinely consulted to monitor the progress of reactions, using aluminum-coated Merck silica gel F254 plates. Purification by column chromatography was achieved by use of Grace Davison Davisil silica column material (LC60A 30-200 micron). Solutions were concentrated using a Heidolph laborota W8 2000 evaporation apparatus and by a high vacuum on a Binder APT line Vacuum Drying Oven. The procedure for a series of similar compounds is given as a general procedure for all within that series, annotated by the numbers of the compounds.

2-(Furan-2-carboxamido) guanidine (2). The mixture of the hydrazide (**1**) (0.1 mol, 12.6 g) and *S*-methylisothiourea sulfate (0.05 mol, 13.9 g) in an 1% aqueous sodium hydroxide solution (400 mL) was stirred at room temperature for 72 hrs. The precipitated solid (**2**), was filtered, washed with ice water, and used in next step without further purification. ^{1}H NMR (400 MHz, DMSO-d_6): δ 10.77 (br s, 1H, NH), 7.56 (s, 1H), 6.88 and 6.76 (2 x s due to dimer formation, 2H, NH_2), 6.64 (d, J = 2.8 Hz, 1H), 6.45 (dd, J = 2.0, 0.8 Hz, 1H).

5-(Furan-2-yl)-2H-1,2,4-triazol-3-amine (3). The guanidine (**2**) (53.6 mmol, 9.0 g) was stirred in a mixture of ethyl acetate and H_2O with a ratio of 1:1 (400 mL) for 3 hrs. After extraction by 150 mL of ethyl acetate twice, the organic layer was washed with H_2O and brine (2 × 100 mL), and dried over anhydrous Na_2SO_4. After removing the solvent, 6.51 g white solid (**4**) was obtained (two-step yield: 54 %). ^{1}H NMR (400 MHz, DMSO-d_6): δ 12.08 (br s, 1H, NH), 7.68 (s, 1H), 6.67 (s, 1H), 6.54 (s, 1H), 6.08 (s, 2H).

2-(Furan-2-yl)-5-(methylthio)-[1,2,4]triazolo[1,5-*a*][1,3,5]triazin-7-amine (4). A mixture of the amine (**3**) (43.4 mmol, 6.5 g) and dimethyl *N*-cyanodithio(imino)carbonate (47.8 mmol, 7.0 g) was heated at 180 ˚C in a stream of nitrogen for 4 hrs and cooled down to room temperature to add 30 mL of a solution of CH_2Cl_2 and CH_3OH with the ratio of 1:1. The mixture was refluxed for another 1.5 hrs and followed by a filtration. The solids were washed by the solution and the solvent was removed under reduced pressure. The residue was purified by column chromatography by eluting with CH_2Cl_2 containing increasing amounts of ethyl acetate (0% - 50%). This gave compound **4** as a pale yellow solid (3.2 g, yield: 30 %). ^{1}H NMR (400 MHz, CD_3OD): δ 7.91 (dd, J = 1.7, 0.7 Hz, 1H), 7.12 (dd, J = 3.4, 0.7 Hz, 1H), 6.70 (dd, J = 3.4, 1.7 Hz, 1H), 2.55 (s, 3H).

2-(Furan-2-yl)-5-(methylsulfonyl)-[1,2,4]triazolo[1,5-*a*][1,3,5]triazin-7-amine (5). A solution of MCPBA (70% strength, 32.5 mmol, 8.0 g) in CH_2Cl_2 (20 mL) was added to a stirred, ice-cooled suspension of the sulfide (R = MeSO) (13.0 mmol, 3.2 g) in CH_2Cl_2 (50 mL). The resulting solution was stirred overnight at room temperature. The solvent was removed and ethanol (70 mL) was added to the residue. The solid was collected by filtration, washed with ethanol, and dried in the vacuum oven to give white solid (R = MeSO2) (3.2 g, yield 88%). 1H NMR (400 MHz, DMSO-d_6): δ 9.81 and 9.48 (2 x s due to dimer formation, 2H, NH_2), 7.98 (dd, J = 1.2, 0.8 Hz, 1H), 7.34 (dd, J = 2.4, 0.8 Hz, 1H), 6.73 (dd, J = 2.4, 1.2 Hz, 1H), 3.35 (s, 3H).

1-(2,4-Dichlophenyl)piperazine (9v). A mixture of **6** (16.7 mmol, 2.0 mL) and piperazine (83.6 mmol, 7.2 g) in 10 mL of *N,N*-dimethylacetamide was heated in the microwave at 165 ˚C for 6.5 hrs after which 6 was consumed, shown by TLC. Water and CH_2Cl_2 was added and the pH value was adjusted to 1 with 1 mol/L HCl (aq.). The aqueous layer was washed three times with CH_2Cl_2 and subsequently basified to pH 12 with 5 mol/L $NaOH_{(aq)}$. After extraction of the basified aqueous layer with CH_2Cl_2 the combined organics were backwashed four times with water, dried over $MgSO_4$ and concentrated *in vacuo* to yield **9v** as yellow oil (2.4 g, yield 61%). ^{1}H NMR (400 MHz, $CDCl_3$): δ 7.36 (d, J = 2.4 Hz, 1H), 7.19 (dd, J = 8.8, 2.4 Hz, 1H), 6.95 (d, J = 8.4 Hz, 1H), 3.06-3.02 (m, 5H, 2 × CH_2 and NH), 2.99-2.96 (m, 4H).

1-(2-Fluoro-4-methoxyphenyl)piperazine hydrochloride (9w). A mixture of bis(2-chloroethyl) amine hydrochloride (9.59 mmol, 1.7 g) (**7**) and 1-butanol (20 mL) was treated slowly with 2-fluoro-4-methoxybenzenamine (9.14 mmol, 1.3 g) at room temperature. After the addition, the mixture was refluxed for 48 hrs and then cooled. The solid was filtered and rinsed with MeOH and Et_2O to give a white solid **9w** (660 mg, yield 29%). ^{1}H NMR (400 MHz, $CDCl_3$): δ 9.21 (br s, 2H, NH and HCl), 7.07-7.02 (m, 1H), 6.86-6.83 (m, 1H), 6.74-6.71 (m, 1H), 3.72 (s, 3H), 3.28-3.20 (m, 4H), 3.14-3.10 (m, 4H).

1-(2,4-Difluorophenyl)piperazine (9x). A mixture of piperazine (24.9 mmol, 2.14 g) and 1-bromo-2,4-difluorobenzene (**8**) (4.1 mmol, 0.8 g), *t*-BuONa (5.8 mmol, 0.56 g), BINAP (0.25 mmol, 0.16 g), and $Pd_2(dba)_3$ (0.083 mmol, 0.048 g) in dry toluene was heated at 110 ˚C under a nitrogen atmosphere for 24 hrs. The mixture was filtered over Celite and rinsed with dichloromethane. The solution was washed

with H_2O and brine (2 × 10 mL), dried over Na_2SO4 and the solvent evaporated *in vacuo*. The residue was purified by silica gel via CH_2Cl_2/CH_3OH, 10:1 to give compound **9x** as pale yellow oil (337 mg, yield 42%). ^{1}H NMR (400 MHz, $CDCl_3$): δ 6.91-6.87 (m, 1H), 6.83-6.78 (m, 2H), 3.06 (t, J = 3.6 Hz, 4H), 3.00-2.97 (m, 4H), 1.80 (s, 1H, NH)

General procedure for preparation of compounds **10a-d**, **10i-x**. The mixture of the appropriate phthalimide-protected alkyl bromide (7.5 mmol), piperazine derivative (5 mmol) and K_2CO_3 (10 mmol) in DMF (5 mL) was stirred at 70 ˚C overnight. The reaction mixture was cooled, washed with H_2O (5 mL) and then extracted with ethyl acetate (3 × 10 mL). The organic phase was then combined, dried over Na_2SO_4 and evaporated *in vacuo* to give the crude product, which was recrystallized from EtOH and/or CH_3OH, or purified by chromatography (petrol ether/ EtOAc).

2-(2-(4-Phenylpiperazin-1-yl)ethyl)isoindoline-1,3-dione (10a). Pale yellow solid was obtained by column chromatography with petrol ether/ EtOAc, 5:1~1:1 (1.5 g, yield 43 %). ^{1}H NMR (400 MHz, $CDCl_3$): δ 7.86-7.80 (m, 4H), 7.25-7.24 (m, 2H), 6.91-6.88 (m, 2H), 6.80 (t, J = 8.1 Hz, 1H), 3.87 (t, J = 6.3 Hz, 2H), 3.15-3.12 (m, 4H), 2.72-2.68 (m, 6H).

2-(3-(4-Phenylpiperazin-1-yl)propyl)isoindoline-1,3-dion (10b). Pale white solid was obtained by recrystallization from EtOH (1.4 g, yield 79 %). ^{1}H NMR (400 MHz, $CDCl_3$): δ 7.89-7.85 (m, 2H), 7.74-7.71 (m, 2H), 7.30-7.24 (m, 2H), 6.90-6.84 (m, 3H), 3.85-3.80 (m, 2H), 3.07 (br s, 4H), 2.57 (br s, 4H), 2.53-2.49 (m, 2H), 1.95-1.92 (m, 2H).

2-(2-(4-Phenylpiperidin-1-yl)ethyl)isoindoline-1,3-dione (10c). Pale white solid was obtained by recrystallization from EtOH (1.3 g, yield 37 %). ^{1}H NMR (400 MHz, $CDCl_3$): δ 7.88-7.85 (m, 2H), 7.76-7.71 (m, 2H), 7.30-7.28 (m, 2H), 7.21-7.18 (m, 3H), 3.87 (t, J = 6.8 Hz, 2H), 3.13 (d, J = 9.6 Hz, 2H), 2.71-2.65 (m, 2H), 2.51-2.44 (m, 1H), 2.19-2.13 (m, 2H), 1.83-1.66 (m, 4H).

***tert*-Butyl-4-(2-(1,3-dioxoisoindolin-2-yl)ethyl)piperazine-1-carboxylate (10d)**. White solid was obtained by silica gel with CH_2Cl_2/EtOAc (10:1~8:1) (558 mg, yield 57 %). ^{1}H NMR (400 MHz, $CDCl_3$): δ 7.79 (dd, J = 5.6, 3.2 Hz, 2H), 7.71 (dd, J = 5.6, 3.2 Hz, 2H), 3.77 (t, J = 6.4 Hz, 2H), 3.30 (t, J = 4.8 Hz, 4H), 2.59 (t, J = 6.4 Hz, 2H), 2.41 (t, J = 4.8 Hz, 4H), 1.39 (s, 9H).

2-(2-(4-(4-Methylphenyl)piperazin-1-yl)ethyl)isoindoline-1,3-dione (10i). Pale white solid was obtained by recrystallization from EtOH (1.5 g, yield 44 %). ^{1}H NMR (400 MHz, $CDCl_3$): δ 7.88-7.82 (m, 2H), 7.75-7.69 (m, 2H), 7.09-7.03 (m, 2H), 6.82 (t, J = 8.8 Hz, 2H), 3.87-3.84 (m, 2H), 3.08-3.06 (m, 4H), 2.70-2.66 (m, 6H), 2.26 (d, J =10 Hz, 3H).

2-(2-(4-(4-Chlorophenyl)piperazin-1-yl)ethyl)isoindoline-1,3-dione (10j). Pale white solid was obtained by recrystallization from EtOH (1.7 g, yield 58 %). ^{1}H NMR (400 MHz, CDCl3): δ 7.84 (dd, J

= 5.2, 2.8 Hz, 2H), 7.7.1 (dd, *J* = 5.2, 2.8 Hz, 2H), 7.17 (dd, *J* = 6.8, 2.4 Hz, 2H), 6.79 (dd, *J* = 6.8, 2.4 Hz, 2H), 3.85 (t, *J* = 6.4 Hz, 2H), 3.08 (t, *J* = 4.8 Hz, 4H), 2.69-2.66 (m, 6H).

2-(2-(4-(4-(Trifluoromethyl)phenyl)piperazin-1-yl)ethyl)isoindoline-1,3-dione (10k). White solid was obtained by recrystallization from EtOH/CH_3OH, 1:1 (985 mg, yield 49 %). ^{1}H NMR (400 MHz, $CDCl_3$): δ 7.83 (dd, *J* = 5.2, 2.8 Hz, 2H), 7.71 (dd, *J* = 5.2, 2.8 Hz, 2H), 7.45 (d, *J* = 8.8 Hz, 2H), 6.88 (d, *J* = 8.8 Hz, 2H), 3.86 (t, *J* = 6.4 Hz, 2H), 3.21 (t, *J* = 4.8 Hz, 4H), 2.71-2.66 (m, 6H).

2-(2-(4-(4-Fluorophenyl)piperazin-1-yl)ethyl)isoindoline-1,3-dione (10l). White solid was obtained by silica gel with Petrol Ether/ EtOAc, 5:1 (1.7 g, yield 49 %). ^{1}H NMR (400 MHz, $CDCl_3$): δ 7.87-7.85 (m, 2H), 7.84-7.82 (m, 2H), 6.98-6.81 (m, 4H), 3.05-3.02 (m, 2H), 3.19-3.07 (m, 4H), 2.70-2.66 (m, 6H).

2-(2-(4-(4-Methoxyphenyl)piperazin-1-yl)ethyl)isoindoline-1,3-dione (10m). Pale white solid was obtained by recrystallization from EtOH (813 mg, yield 45 %). ^{1}H NMR (400 MHz, $CDCl_3$): δ 7.84 (dd, *J* = 5.2, 2.8 Hz, 2H), 7.71 (dd, *J* = 5.2, 2.8 Hz, 2H), 6.88-6.86 (m, 2H), 6.82-6.80 (m, 2H), 3.88 (t, *J* = 6.4 Hz, 2H), 3.75 (s, 3H), 3.04-3.02 (m, 4H), 2.70-2.69 (m, 6H).

2-(2-(4-([1,1'-Biphenyl]-4-yl)piperazin-1-yl)ethyl)isoindoline-1,3-dione (10n). Pale white solid was obtained by recrystallization from EtOH (1.0 g, yield 55 %). ^{1}H NMR (400 MHz, $CDCl_3$): δ 7.84 (dd, *J* = 5.2, 2.8 Hz, 2H), 7.72 (dd, *J* = 5.2, 2.8 Hz, 2H), 7.54 (d, *J* = 7.6 Hz, 2H), 7.49 (d, *J* = 8.8 Hz, 2H), 7.39 (t, *J* = 7.6 Hz, 2H), 7.25 (s, 1H), 6.95 (d, *J* = 8.8 Hz, 2H), 3.87 (t, *J* = 6.8 Hz, 2H), 3.19-3.17 (m, 4H), 2.72-2.70 (m, 6H).

2-(2-(4-(2-Methylphenyl)piperazin-1-yl)ethyl)isoindoline-1,3-dione (10o). Pale white solid was obtained by column chromatography (CH_2Cl_2 - 2% MeOH/CH_2Cl_2) (1.9 g, yield 57 %). ^{1}H NMR (400 MHz, $CDCl_3$): δ 7.86-7.83 (m, 2H), 7.75-7.68 (m, 2H), 7.17-7.11 (m, 2H), 6.99-6.92 (m, 2H), 3.87 (d, *J* = 6.4 Hz, 2H), 2.90-2.84 (m, 4H), 2.76-2.68 (m, 6H), 2.29 (s, 3H).

2-(2-(4-(2-Methoxyphenyl)piperazin-1-yl)ethyl)isoindoline-1,3-dione (10p). Pale white solid was obtained by column chromatography (CH_2Cl_2 - 2% MeOH/CH_2Cl_2) (2.49 g, yield 60 %). ^{1}H NMR (400 MHz, $CDCl_3$): δ 7.86-7.83 (m, 2H), 7.73-7.70 (m, 2H), 7.00-6.96 (m, 1H), 6.92- 6.87 (m, 2H), 6.84 (d, *J* = 7.6 Hz, 1H), 3.87-3.84 (m, 5H), 3.10-2.93 (m, 4H), 2.74-2.67 (m, 6H).

2-(2-(4-(2-Chlorophenyl)piperazin-1-yl)ethyl)isoindoline-1,3-dione (10q). Pale white solid was obtained by column chromatography (CH_2Cl_2 – 2% MeOH/CH_2Cl_2) (2.11 g, yield 64%). ^{1}H NMR (400 MHz, $CDCl_3$): δ 7.88-7.83 (m, 2H), 7.74-7.70 (m, 2H), 7.33 (dd, *J* = 8.0, 1.6 Hz, 1H), 7.19 (td, *J* = 8.0, 1.6 Hz, 1H), 7.01 (dd, *J* = 8.0, 1.2 Hz, 1H), 6.94 (td, *J* = 7.6, 1.2 Hz, 1H), 3.87 (d, *J* = 6.8 Hz, 2H), 3.10-2.94 (m, 4H), 2.81-2.63 (m, 6H).

2-(2-(4-(2-Fluorophenyl)piperazin-1-yl)ethyl)isoindoline-1,3-dione (10r). Pale white solid was obtained by recrystallization from EtOH (1.97 g, yield 74%). ^{1}H NMR (400 MHz, $CDCl_3$): δ 7.87-7.83 (m, 2H), 7.74-7.70 (m, 2H), 7.21-7.17 (m, 2H), 6.97-6.93 (m, 2H), 3.90-3.84 (m, 2H), 3.10-3.00 (m, 4H), 2.65-2.52 (m, 6H).

2-(2-(4-(3-Fluorophenyl)piperazin-1-yl)ethyl)isoindoline-1,3-dione (10s). Pale white solid was obtained by recrystallization from EtOH (1.97 g, yield 74%). ^{1}H NMR (400 MHz, $CDCl_3$): δ 7.83-7.82 (m, 2H), 7.71-7.67 (m, 2H), 7.18-7.12 (m, 1H), 6.64-6.63 (m, 1H), 6.55-6.47 (m, 2H), 3.86-3.83 (m, 2H), 3.15-3.10 (m, 4H), 2.75-2.60 (m, 6H).

2-(2-(4-(2,4-Dimethylphenyl)piperazin-1-yl)ethyl)isoindoline-1,3-dione (10t). Pale white solid (852 mg, yield 45%) was obtained by column purification (2% MeOH/CH_2Cl_2). ^{1}H NMR (400 MHz, $CDCl_3$): δ 7.88-7.83 (m, 2H), 7.75-7.69 (m, 2H), 6.98 (s, 1H), 6.94 (d, J = 8.0 Hz, 1H), 6.89 (d, J = 8.4 Hz, 1H), 3.86 (t, J = 6.8 Hz, 2H), 2.90-2.81 (m, 4H), 2.73-2.68 (m, 6H).

2-(2-(4-(3,4-Dichlorophenyl)piperazin-1-yl)ethyl)isoindoline-1,3-dione (10u). Pale white solid was obtained by recrystallization from EtOH.(1.78 g, yield 88 %). ^{1}H NMR (400 MHz, $CDCl_3$): δ 7.85-7.83 (m, 2H), 7.72-7.70 (m, 2H), 7.23 (s, 1H), 6.92 (d, J = 2.8 Hz, 1H), 6.71 (dd, J = 8.8, 2.8 Hz, 1H), 3.87-3.84 (m, 2H), 3.11-3.08(m, 4H), 2.71-2.65 (m, 6H).

2-(2-(4-(2,4-dichlorophenyl)piperazin-1-yl)ethyl)isoindoline-1,3-dione (10v). Pale white solid (509 mg, yield 29%) was obtained by column purification (1% MeOH/CH_2Cl_2). ^{1}H NMR (400 MHz, $CDCl_3$): δ 7.88-7.83 (m, 2H), 7.74-7.70 (m, 2H), 7.33 (d, J = 2.4 Hz, 1H), 7.15 (dd, J = 8.4, 2.4 Hz, 1H), 6.91 (d, J = 8.4 Hz, 1H), 3.86 (t, J = 6.8 Hz, 2H), 3.06-2.95 (m, 4H), 2.78-2.68 (m, 6H).

2-(2-(4-(2-Fluoro-4-methoxyphenyl)piperazin-1-yl)ethyl)isoindoline-1,3-dione (10w). Pale white solid (859 mg, yield 54%) was obtained by column chromatography (CH_2Cl_2-2% MeOH/CH_2Cl_2). ^{1}H NMR (400 MHz, $CDCl_3$): δ 7.87-7.83 (m, 2H), 7.74-7.70 (m, 2H), 6.87 (t, J = 9.2 Hz, 1H), 6.65-6.58 (m, 2H), 3.86 (t, J = 6.8 Hz, 2H), 3.74 (s, 3H), 3.07-2.95 (m, 4H), 2.72-2.69 (m, 6H).

2-(2-(4-(2,4-Difluorophenyl)piperazin-1-yl)ethyl)isoindoline-1,3-dione (10x). White solid was obtained by silica gel with petrol ether/EtOAc, 20:1~5:1, (389 mg, yield 65 %). ^{1}H NMR (400 MHz, $CDCl_3$): δ 7.81-7.79 (m, 2H), 7.67-7.65 (m, 2H), 6.84-6.78 (m, 1H), 6.75-6.69 (m, 2H), 3.97 (m, 2H), 2.93 (m, 4H), 2.66 (m, 6H).

General Procedure for Preparation of Compounds **11a-d**, **11i-x**. Hydrazine hydrate was added in excess (1 ~ 5 mL) to a solution of isoindoline-1,3-dione (3 mmol) in EtOH (25 mL) and the mixture was stirred at 70 ˚C overnight. The solvent was removed *in vacuo* and EtOAc was added to the residue. The solids were

filtered, dried over Na_2SO_4 and evaporated *in vacuo* to give the crude product as a pale yellow oil or solid. The crude product is used in the next step without further purification.

General Procedure for Preparation of Compounds **12a-x**. The mixture of the related amine (0.75 mmol), the sulfone / sulfoxide mixture (**5**) (0.50 mmol) and Et_3N (1.0 mmol) was dissolved in CH_3CN and refluxed overnight. After removing the solvent *in vacuo*, EtOAc was added and the organic phase was washed with H_2O and brine (2 × 10 mL), dried over Na_2SO_4 and evaporated. The residue was purified by column chromatography using silica gel and EtOAc or EtOAc/MeOH to afford a white to off-white solid.

2-(Furan-2-yl)-*N*^{5}-(2-(4-phenylpiperazin-1-yl)ethyl)-[1,2,4]triazolo[1,5-*a*][1,3,5]triazine-5,7-diamine (12a). Eluted with EtOAc/MeOH, 10:1 to afford the title compound as white powder (55 mg, yield: 14%). ^{1}H NMR (400 MHz, MeOD): δ 7.68 (s, 1H), 7.22 (t, J = 8.4 Hz, 2H), 7.12 (d, J = 3.2 Hz, 1H), 6.96 (d, J = 8.4 Hz, 2H), 6.84-6.81 (m, 1H), 6.60 (d, J = 1.6 Hz, 1H), 3.61-3.60 (m, 2H), 3.20 (t, J = 4.8 Hz, 4H), 2.72 (t, J = 4.8 Hz, 4H), 2.68-2.67 (m, 2H). ^{13}C NMR (101 MHz, DMSO-d_6): 161.6, 159.7, 156.3, 151.5, 150.5, 146.7, 145.1, 129.4, 119.2, 115.8, 112.4, 112.1, 57.1, 53.2, 48.7, 38.5. HRMS (ESI) *m/z* [*M*+H]$^+$ calcd for $C_{20}H_{24}N_9O^+$: 406.2026, found: 406.2092; HPLC: ret. time =11.96 min., purity = 96.7%.

2-(Furan-2-yl)-*N*^{5}-(3-(4-phenylpiperazin-1-yl)propyl)-[1,2,4]triazolo[1,5-*a*][1,3,5]triazine-5,7-diamine (12b). Eluted with EtOAc/MeOH, 10:1 to afford the title compound as white powder (87 mg, yield: 41%). ^{1}H NMR (400 MHz, DMSO-d_6): δ 8.42 and 8.13 (2 x s due to dimer formation, 2H, NH_2), 7.86 (s, 1H), 7.55 and 7.44 (2 x t due to dimer formation, J = 5.2 Hz, 1H, NH), 7.19 (t, J = 8.0 Hz, 2H), 7.04-7.03 (m, 1H), 6.91 (d, J = 8.0 Hz, 2H), 6.75 (t, J = 6.8 Hz, 1H), 6.66 (s, 1H), 3.30-3.29 (m, 4H), 3.12-3.10 (m, 6H), 2.40-2.36 (m, 2H), 1.74-1.71 (m, 2H). ^{13}C NMR (101 MHz, DMSO-d_6): δ 162.0, 161.6, 159.7, 156.3, 151.5, 151.1, 150.4, 146.7, 145.1, 129.4, 122.9, 119.1, 115.7, 112.4, 112.1, 108.7, 56.1, 56.0, 53.3, 48.6, 26.5. HRMS (ESI) *m/z* [*M*+H]$^+$ calcd for $C_{21}H_{26}N_9O^+$: 420.2182, found 420.2253; HPLC: ret. time = 11.98 min., purity = 97.8 %.

2-(Furan-2-yl)-*N*^{5}-(2-(4-phenylpiperidin-1-yl)ethyl)-[1,2,4]triazolo[1,5-*a*][1,3,5]triazine-5,7-diamine (12c). Eluted with EtOAc/MeOH, 3:2 to afford the title compound as white powder (29 mg, yield: 14%). ^{1}H NMR (400 MHz, DMSO-d_6): 8.46 and 8.21 (2 x s due to dimer formation, 2H, NH_2), 7.88 (s, 1H), 7.35 and 7.33 (2 x t due to dimer formation, J = 7.2 Hz, 1H, NH), 7.31-7.22 (m, 4H), 7.20-7.17 (m, 1H), 7.07 (d, J = 3.6 Hz, 1H), 6.69-6.68 (m, 1H), 3.45-3.42 (m, 2H), 3.05-3.02 (m, 2H), 2.52-2.51 (m, 2H), 2.49-2.44 (m, 1H), 2.12-2.07(m, 2H), 1.76-1.63 (m, 4H). ^{13}C NMR (101 MHz, DMSO-d_6): 161.6, 159.7, 156.3, 150.5, 146.7, 146.6, 145.1, 128.8, 127.2, 126.4, 112.4, 112.1, 57.4, 54.3, 42.3, 38.6, 33.5. HRMS (ESI) *m/z* [*M*+H]$^+$ calcd for $C_{21}H_{25}N_8O^+$: 405.2073, found: 405.2142; HPLC: ret. time = 12.20 min., purity = 99.5%.

***tert*-Butyl-4-(2-(7-amino-2-(furan-2-yl)-[1,2,4]triazolo[1,5-*a*][1,3,5]triazin-5-ylamino)ethyl)**

piperazine-1-carboxylate (12d). Eluted with petrol ether/EtOAc from 1:1 to 1:9 to afford the title compound as white powder (20 mg, yield: 31%). ^{1}H NMR (400 MHz, MeOD): δ 7.69 (d, J = 0.8 Hz, 1H), 7.12 (d, J = 3.2 Hz, 1H), 6.61 (dd, J = 3.2 Hz, 0.8 Hz, 1H), 3.60-3.57 (m, 2H), 3.46-3.45 (m, 4H), 2.63-2.62 (m, 2H), 2.52-2.50 (m, 4H), 1.46 (s, 9H). HRMS (ESI) *m/z* [*M*+H]$^+$ calcd for $C_{19}H_{28}N_9O_3^+$: 430.2237, found: 430.2308; HPLC: ret. time = 11.86 min., purity = 96.3%.

2-(Furan-2-yl)-*N*^{5}-(2-(piperazin-1-yl)ethyl)-[1,2,4]triazolo[1,5-*a*][1,3,5]triazine-5,7-diamine di-trifluoroacetate (12e). The Boc-protected compound (**12d**) (20 mg) was dissolved in a CH_2Cl_2/TFA mixture, 1:1 (5 mL). The mixture was stirred at room temperature for 24 hrs. A brown solid was obtained (13 mg, yield: 82%). ^{1}H NMR (400 MHz, DMSO-d_6): 8.41 and 8.16 (2 x s due to dimer formation, 2H, NH_2), 7.86 (s, 1H), 7.30 (br s, 1H, NH), 7.04 (s, 1H), 6.67 (s, 1H), 3.50 (br s, 2H), 3.04 (br s, 4H), 2.60 (br s, 4H), 2.50 (br s, 2H). ^{13}C NMR (101 MHz, DMSO-d_6): 161.7, 159.6, 150.6, 146.7, 145.4, 112.4, 112.1, 108.6, 56.9, 50.3, 43.7, 38.2. HRMS (ESI) *m/z* [*M*+H]+ calcd for $C_{18}H_{22}F_6N_9O_5^+$: 557.1570, found: 330.1786 ([*M*+H$^+$]-2TFA); HPLC: ret. time = 11.92 min., purity = 98.9 %.

2-(Furan-2-yl)-*N*^{5}-(2-(4-methylpiperazin-1-yl)ethyl)-[1,2,4]triazolo[1,5-*a*][1,3,5]triazine-5,7-diamine (12f). Eluted with EtOAc/MeOH, 3:2 to afford the title compound as white powder (61 mg, yield: 35%). ^{1}H NMR (400 MHz, DMSO-d_6): 8.16 (2 x s due to dimer formation, 2H, NH_2), 7.81 (s, 1H), 7.24 and 7.16 (2 x t due to dimer formation, J = 5.6 Hz, 1H, NH), 7.00-6.99 (m, 1H), 6.62-6.61 (m, 1H), 3.33-3.32 (m, 2H), 2.46-2.45 (m, 2H), 2.42-2.36 (m, 4H), 2.27-2.24 (m, 4H), 2.07(s, 3H). ^{13}C NMR (101 MHz, DMSO-d_6): 161.6, 159.7, 156.3, 150.5, 146.6, 145.1, 129.6, 112.4, 112.1, 57.1, 55.2, 53.2, 46.2, 38.5. HRMS (ESI) *m/z* [*M*+H]$^+$ calcd for $C_{24}H_{34}N_9O^+$: 344.1869, found: 344.1942; HPLC: ret. time = 11.70 min., purity = 99.2%.

***N*^{5}-(2-(4-benzylpiperazin-1-yl)ethyl)-2-(furan-2-yl)-[1,2,4]triazolo[1,5-*a*][1,3,5]triazine-5,7-diamine (12g).** Eluted with EtOAc/MeOH, 3:2 to afford the title compound as white powder (34 mg, yield: 16%). ^{1}H NMR (400 MHz, DMSO-d_6): 8.39 and 8.13 (2 x s for due to dimer formation, 2H, NH_2), 7.82 (s, 1H), 7.28-7.17 (m, 6H), 7.01-7.00 (m, 1H), 6.63-6.62 (m, 1H), 3.39 (s, 2H), 3.34-3.33 (m,2H), 2.47-2.46 (m, 2H), 2.44-2.41 (m, 4H), 2.33-2.31 (m, 4H). ^{13}C NMR (101 MHz, DMSO-d_6): 161.6, 159.7, 156.3, 150.5, 146.6, 145.1, 138.7, 129.3, 128.6, 127.3, 112.4, 112.1, 62.6, 57.6, 57.1, 53.3, 53.1, 46.2, 38.5. HRMS (ESI) *m/z* [*M*+H]$^+$ calcd for $C_{21}H_{25}N_8O^+$: 420.2181, found: 420.2254; HPLC: ret. time = 12.14 min., purity = 99.6%.

2-(Furan-2-yl)-*N*^{5}-(2-(piperidin-1-yl)ethyl)-[1,2,4]triazolo[1,5-*a*][1,3,5]triazine-5,7-diamine (12h). Washed with CH_3CN and CH_2Cl_2 to afford the title compound as white powder (63 mg, yield: 43%). ^{1}H NMR (400 MHz, MeOD): δ 7.69 (s, 1H), 7.12 (d, J = 8.4 Hz, 1H), 6.61-6.60 (m, 1H), 3.57 (t, J = 6.8 Hz, 2H), 2.59-2.58 (m, 2H), 2.52-2.51 (m, 4H), 1.64-1.60 (m, 4H), 1.49-1.48 (m, 2H). ^{13}C NMR (101 MHz, DMSO-d_6): 161.6, 159.7, 156.3, 150.5, 146.7, 145.1, 112.4, 112.1, 57.8, 54.6, 38.6, 26.1, 24.5. HRMS (ESI) *m/z* [*M*+H]$^+$ calcd for $C_{15}H_{21}N_8O^+$: 329.1760, found: 329.1832; HPLC: ret.

time =11.31 min., purity = 96.3%.

2-(Furan-2-yl)-N^5-(2-(4-(4-methylphenyl)piperazin-1-yl)ethyl)-[1,2,4]triazolo[1,5-*a*][1,3,5]triazine-5,7-di-amine (12i). Eluted with EtOAc/MeOH, 5:1, to afford the title compound as white powder (65 mg, yield: 31%). ^{1}H NMR (400 MHz, DMSO-d_6): 8.42 and 8.19 (2 x s due to dimer formation, 2H, NH_2), 7.86 (s, 1H), 7.35 and 7.28 (2 x s due to dimer formation, 1H, NH), 7.05 (s, 1H), 7.01-7.00 (m, 2H), 6.84-6.82 (m,2H), 6.67 (s, 1H), 3.42 (br s, 2H), 3.06 (br s, 4H), 2.56 (br s, 2H), 2.50 (br s, 4H), 2.18 (s, 3H). ^{13}C NMR (101 MHz, DMSO-d_6): 161.6, 160.0, 156.3, 150.5, 149.4, 146.6, 145.1, 129.8, 128.0, 116.0, 112.4, 112.1, 57.1, 53.3, 49.1, 38.5, 20.5. HRMS (ESI) *m/z* [*M*+H]$^+$ calcd for $C_{21}H_{26}N_9O^+$: 420.2182, found: 420.2253; HPLC: ret. time = 12.16 min., purity = 96.0%.

***N*^{5}-(2-(4-(4-chlorophenyl)piperazin-1-yl)ethyl)-2-(furan-2-yl)-[1,2,4]triazolo[1,5-*a*][1,3,5]triazine-5,7-diamine (12j).** Eluted with EtOAc/MeOH, 10:1, to afford the title compound as white powder (30 mg, yield: 14%). ^{1}H NMR (400 MHz, DMSO-d_6): 8.41 and 8.19 (2 x s due to dimer formation, 2H, NH_2), 7.86 (s, 1H), 7.35 and 7.28 (2 x s due to dimer formation, 1H, NH), 7.22-7.20 (m, 2H), 7.05 (s, 1H), 6.93 (br s, 2H), 6.67 (s, 1H), 3.42 (br s. 2H), 3.12 (br s, 4H), 2.56 (br s, 2H), 2.50 (br s, 4H). ^{13}C NMR (101 MHz, DMSO-d_6): 161.9, 159.8, 156.4, 150.3, 146.8, 145.1, 129.0, 122.7, 117.2, 112.4, 112.1, 57.1, 53.0, 48.5, 38.5. HRMS (ESI) *m/z* [*M*+H]$^+$ calcd for $C_{20}H_{23}ClN_9O^+$: 440.1636, found: 440.1707; HPLC: ret. time = 12.41 min., purity = 95.0%.

***N*^{5}-(2-(4-(4-(trifluoromethyl)phenyl)piperazin-1-yl)ethyl)-2-(furan-2-yl)-[1,2,4]triazolo[1,5-*a*][1,3,5]triazine-5,7-diamine (12k).** Eluted with EtOAc/MeOH, 5:1, to afford the title compound as white powder (50 mg, yield: 21%). ^{1}H NMR (400 MHz, DMSO-d_6): 8.43 and 8.19 (2 x s due to dimer formation, 2H, NH_2), 7.86 (s, 1H), 7.49 (d, J = 8.8 Hz, 2H) 7.37 and 7.30 (2 x s due to dimer formation, 1H, NH), 7.06-7.05 (m, 1H), 7.05-7.04 (m, 2H), 6.67 (s, 1H), 3.43-3.42 (m, 2H), 3.27-3.25 (m, 4H), 2.57-2.53 (m, 6H). ^{13}C NMR (101 MHz, DMSO-d_6): 161.6, 159.7, 156.3, 153.7, 150.5, 146.7, 145.1, 126.6, 126.5, 118.4, 118.0, 114.6, 112.4, 112.1, 57.0, 53.0, 47.4, 38.5. HRMS (ESI) *m/z* [*M*+H]$^+$ calcd for $C_{21}H_{23}F_3N_9O^+$: 474.1899, found: 474.1969; HPLC: ret. time = 12.52 min., purity = 95.0%.

***N*^{5}-(2-(4-(4-fluorophenyl)piperazin-1-yl)ethyl)-2-(furan-2-yl)-[1,2,4]triazolo[1,5-*a*][1,3,5]triazine-5,7-diamine (12l).** Eluted with EtOAc/MeOH, 10:1, to afford the title compound as white powder (45 mg, yield: 21%). ^{1}H NMR (400 MHz, DMSO-d_6): 8.19 and 8.12 (2 x s for due to dimer formation, 2H, NH_2), 7.86 (s, 1H), 7.35 and 7.28 (2 x s due to dimer formation, 1H, NH), 7.05-7.01 (m, 2H), 7.00 (s, 1H), 6.94-6.91 (m, 2H), 6.67 (s,1H), 3.43-3.41 (m. 2H), 3.06 (br s, 4H), 2.57-2.53 (m, 6H). ^{13}C NMR (101 MHz, DMSO-d_6): 161.6, 161.1, 159.2, 156.7, 156.1, 155.8, 155.1, 150.7, 150.0, 147.9, 146.2, 144.6, 117.0, 116.9, 115.3, 115.1, 111.9, 111.6, 57.0, 56.6, 52.7, 49.0, 38.4, 38.0. HRMS (ESI) *m/z* [*M*+H]$^+$ calcd for $C_{20}H_{23}FN_9O^+$: 424.1931, found: 424.2002; HPLC: ret. time = 12.08 min., purity = 97.2%.

2-(Furan-2-yl)-*N*^{5}-(2-(4-(4-methoxyphenyl)piperazin-1-yl)ethyl)-[1,2,4]triazolo[1,5-*a*][1,3,5] triazine-5,7-diamine (12m). Eluted with EtOAc/MeOH, 5:1, to afford the title compound as white powder (64 mg, yield: 29%). ^{1}H NMR (400 MHz, DMSO-d_6): 8.44 and 8.20 (2 x s for due to dimer formation, 2H, NH_2), 7.86 (s, 1H), 7.34 and 7.27 (2 x s due to dimer formation, 1H, NH), 7.05 (d, J = 2.4 Hz, 1H), 6.87 (d, J = 8.8 Hz, 2H), 6.79 (d, J = 8.8 Hz, 2H), 6.67 (s, 1H), 3.66 (s, 3H), 3.42-3.39 (m, 2H), 3.00 (br s, 4H), 2.56-2.52 (m, 6H). ^{13}C NMR (101 MHz, DMSO-d_6): 161.6, 159.7, 156.3, 153.3, 150.5, 146.6, 145.9, 145.1, 117.7, 114.7, 112.4, 112.1, 57.1, 55.6, 53.3, 50.0, 38.5. HRMS (ESI) *m/z* [*M*+H]$^+$ calcd for $C_{21}H_{26}N_9O_2^+$: 436.2131, found: 436.2202; HPLC: ret. time = 11.75 min., purity = 95.6%.

***N*^{5}-(2-(4-([1,1'-biphenyl]-4-yl)piperazin-1-yl)ethyl)-2-(furan-2-yl)[1,2,4]triazolo[1,5-*a*][1,3,5] trizaine-5,7-diamine (12n).** Eluted with EtOAc/MeOH, 10:1, to afford the title compound as white powder (55 mg, yield: 23%). ^{1}H NMR (400 MHz, DMSO-d_6): 8.53 (s, 1H), 8.21 (br s, 2H, NH_2), 7.87 (s, 1H), 7.60-7.52 (m, 3H), 7.40-7.39 (m, 2H), 7.30-7.27 (m, 1H), 7.06-7.01 (m, 3H), 6.68 (s, 1H), 4.31 (m, 2H), 3.49-3.43 (m, 2H), 3.20-3.19 (m, 4H), 2.60-2.58 (m, 4H). ^{13}C NMR (101 MHz, DMSO-d_6): 161.6, 159.7, 156.3, 150.8, 150.5, 146.6, 146.5, 145.1, 140.5, 130.7, 129.3, 127.6, 126.8, 126.3, 115.9, 112.4, 112.1, 57.1, 53.2, 48.4, 38.5. HRMS (ESI) *m/z* [*M*+H]$^+$ calcd for $C_{26}H_{28}N_9O^+$: 482.2339, found: 482.2408; HPLC: ret. time = 11.98 min., purity = 97.8 %.

2-(furan-2-yl)-*N*^{5}-(2-(4-(2-methyphenyl)piperazin-1-yl)ethyl)-[1,2,4]triazolo[1,5-*a*][1,3,5]triazine-5,7-diamine (12o). Eluted with EtOAc/MeOH, 3:2 to afford the title compound as white powder (116 mg, yield: 55%). ^{1}H NMR (400 MHz, DMSO-d_6): 8.44 and 8.19 (2 x s due to dimer formation, 2H, NH_2), 7.88 (s, 1H), 7.35 and 7.27 (2 x s due to dimer formation, 1H, NH), 7.16-7.11 (m, 2H), 7.06 (s, 1H), 7.02 (d, J = 7.6 Hz, 1H), 6.95 (t, J = 7.2 Hz, 1H), 6.68 (s, 1H), 3.46-3.43 (m, 2H), 2.90-2.78 (m, 4H), 2.61-2.55 (m, 6H), 2.24 (s, 3H). ^{13}C NMR (101 MHz, DMSO-d_6): 161.6, 161.2, 159.2, 155.9, 151.3, 150.1, 146.2, 144.7, 131.7, 130.8, 126.5, 122.8, 118.7, 111.9, 111.7, 56.7, 53.3, 51.3, 38.0, 17.6. HRMS (ESI) *m/z* [*M*+H]$^+$ calcd for $C_{21}H_{26}N_9O^+$: 420.2182, found: 420.2252 ; HPLC: ret. time = 12.37 min., purity = 99.6%.

2-(furan-2-yl)-*N*^{5}-(2-(4-(2-methoxyphenyl)piperazin-1-yl)ethyl)-[1,2,4]triazolo[1,5-*a*][1,3,5] triazine-5,7-diamine (12p). Eluted with EtOAc/MeOH, 3:2 to afford the title compound as white powder (130 mg, yield: 60%). ^{1}H NMR (400 MHz, DMSO-d_6): 8.44 and 8.20 (2 x s due to dimer formation, 2H, NH_2), 7.86 (s, 1H), 7.40 and 7.27 (2 x s due to dimer formation, 1H, NH), 7.06 (s, 1H), 6.91-6.90 (m, 2H), 6.85-6.84 (m, 2H), 6.67 (s, 1H), 3.79 (s, 3H), 3.43-3.42 (m, 2H), 2.95-2.94 (m, 4H), 2.57-2.50 (m, 6H). ^{13}C NMR (101 MHz, DMSO-d_6): 161.2, 159.2, 155.9, 152.0, 150.0, 146.2, 144.7, 141.3, 122.3, 120.8, 117.9, 111.9, 111.8, 111.6, 56.7, 55.3, 53.1, 50.1, 38.3. HRMS (ESI) *m/z* [*M*+H]$^+$ calcd for $C_{21}H_{26}N_9O_2^+$: 436.2131, found: 436.2007; HPLC: ret. time = 12.08 min., purity = 99.9%.

***N*^{5}-(2-(4-(2-chlorophenyl)piperazin-1-yl)ethyl)-2-(furan-2-yl)-[1,2,4]triazolo[1,5-*a*][1,3,5] triazine-5,7-diamine (12q).** Eluted with EtOAc/MeOH, 3:2 to afford the title compound as white powder (113 mg, yield: 51%). ^{1}H NMR (400 MHz, DMSO-d_6): 8.42 and 8.18 (2 x s due to dimer formation, 2H, NH_2), 7.87 (s, 1H), 7.47-7.38 (dd, J = 7.6, 1.2 Hz, 1H), 7.35-7.25 (m, 2H), 7.15 (d, J = 8.0 Hz, 1H), 7.05-7.01 (m, 2H), 6.68-6.67 (m, 1H), 3.45-3.40 (m, 2H), 2.98-2.97 (m, 4H), 2.61-2.49 (m, 6H). ^{13}C NMR (101 MHz, DMSO-d_6): 161.2, 159.2, 155.9, 150.0, 149.1, 146.2, 144.7, 130.3, 128.1, 127.6, 123.8, 120.8, 118.7, 111.9, 111.7, 56.6, 52.9, 50.9, 38.0. HRMS (ESI) *m/z* [*M*+H]$^+$ calcd for $C_{20}H_{23}ClN_9O^+$: 440.1636, found: 440.1706 ; HPLC: ret. time = 12.27 min., purity = 99.5%.

***N*^{5}-(2-(4-(2-fluorophenyl)piperazin-1-yl)ethyl)-2-(furan-2-yl)-[1,2,4]triazolo[1,5-*a*][1,3,5]triazine-5,7-diamine (12r).** Eluted with EtOAc/MeOH, 10:1 to afford the title compound as white powder (66 mg, yield: 31%). ^{1}H NMR (400 MHz, DMSO-d_6): 8.46 and 8.21 (2 x s due to dimer formation, 2H, NH_2), 7.86 (s, 1H), 7.35 and 7.14 (2 x t due to dimer formation, J = 5.6 Hz, 1H, NH), 7.14-6.92 (m, 5H), 6.68-6.67 (m, 1H), 3.44-3.43 (m, 2H), 3.02-3.01 (m, 4H), 2.60-2.59 (m, 4H), 2.57-2.53 (m, 2H). ^{13}C NMR (101 MHz, DMSO-d_6): 161.6, 159.7, 156.6, 154.2, 150.5, 146.6, 145.1, 140.3, 125.3, 125.2, 122.7, 122.6, 119.6, 116.5, 116.3, 112.4, 112.1, 57.0, 53.3, 50.6, 50.5, 38.4. HRMS (ESI) *m/z* [*M*+H]$^+$ calcd for $C_{20}H_{23}FN_9O^+$: 424.1931, found: 424.2002; HPLC: ret. time = 12.00 min., purity = 95.6%.

***N*^{5}-(2-(4-(3-fluorophenyl)piperazin-1-yl)ethyl)-2-(furan-2-yl)-[1,2,4]triazolo[1,5-*a*][1,3,5]triazine-5,7-diamine (12s).** Eluted with EtOAc/MeOH, 3:2 to afford the title compound as white powder (96 mg, yield: 45%). ^{1}H NMR (400 MHz, DMSO-d_6): 8.44 and 8.19 (2 x s due to dimer formation, 2H, NH_2), 7.86 (s, 1H), 7.37 and 7.27 (2 x t due to dimer formation, J = 5.2 Hz, 1H, NH), 7.22-7.16 (m, 1H), 7.05-7.04 (d, J = 3.2 Hz, 1H), 6.75-6.66 (m, 3H), 6.54-6.49 (m, 1H), 3.44-3.39 (m, 2H), 3.15 (br s, 4H), 2.55-2.52 (m, 6H). ^{13}C NMR (101 MHz, DMSO-d_6): 164.9, 162.5, 162.0, 161.6, 159.7, 156.6, 156.3, 153.3, 153.2, 151.1, 150.5, 146.6, 145.1, 130.8, 130.7, 112.4, 112.1, 111.2, 105.1, 104.9, 102.2, 102.0, 57.5, 57.0, 53.0, 48.1, 38.9, 38.4. HRMS (ESI) *m/z* [*M*+H]$^+$ calcd for $C_{20}H_{23}FN_9O^+$: 424.1931, found 424.2002; HPLC: ret. time = 12.06 min., purity = 98.5%.

***N*^{5}-(2-(4-(2,4-dimethylphenyl)piperazin-1-yl)ethyl)-2-(furan-2-yl)-[1,2,4]triazolo[1,5-*a*][1,3,5] triazine-5,7-diamine (12t).** Eluted with EtOAc/MeOH, 5:1 to afford the title compound as white powder (128 mg, yield: 59%). ^{1}H NMR (400 MHz, DMSO-d_6): 8.40 and 8.17 (2 x s due to dimer formation, 2H, NH_2), 7.88 (s, 1H), 7.33 and 7.26 (2 x t, J = 5.2 Hz, 1H, NH), 7.06-7.05 (m, 1H), 6.99-6.90 (m, 4H), 6.68 (s, 1H), 3.43 (t, J = 6.0 Hz, 2H), 2.80 (br s, 4H), 2.59-2.51 (m, 6H), 2.20 (s, 6H). ^{13}C NMR (101 MHz, DMSO-d_6): 161.2, 159.2, 155.9, 150.0, 148.9, 146.2, 144.6, 131.5, 131.4, 126.9, 118.6, 111.9, 111.6, 56.7, 53.3, 51.5, 38.0, 20.3, 17.4. HRMS (ESI) *m/z* [*M*+H]$^+$ calcd for $C_{22}H_{28}N_9O^+$: 434.24113, found: 434.24088; HPLC: ret. time = 7.98 min., purity = 99.3%.

***N*^{5}-(2-(4-(3,4-dichlorophenyl)piperazin-1-yl)ethyl)-2-(furan-2-yl)-[1,2,4]triazolo[1,5-*a*] [1,3,5]-triazine-5,7-diamine (12u).** Eluted with EtOAc/MeOH, 10:1, to afford the title compound as

white powder (128 mg, yield: 59%). ^{1}H NMR (400 MHz, DMSO-d_6): 8.44 and 8.20 (2 x s due to dimer formation, 2H, NH_2), 7.87 (s, 1H), 7.38 (d, J = 8.8 Hz, 1H), 7.29 (t, J = 5.2 Hz, 1H, NH), 7.12 (d, J = 2.8 Hz, 1H), 7.05 (d, J = 3.2 Hz, 1H), 6.94 (dd, J = 9.2, 2.8 Hz, 1H), 6.68 (dd, J = 3.2, 1.6 Hz, 1H), 3.45-3.43 (m, 2H), 3.18 (br s, 4H), 2.55-2.51 (m, 6H). ^{13}C NMR (101 MHz, DMSO-d_6): 161.6, 159.7, 156.3, 151.2, 150.5, 146.7, 145.1, 131.9, 130.9, 120.0, 116.6, 115.7, 112.4, 112.1, 57.0, 52.9, 48.0, 38.4. HRMS (ESI) *m/z* [*M*+H]$^+$ calcd for $C_{20}H_{22}Cl_2N_9O^+$: 474.1246, found: 474.1317; HPLC: ret. time = 12.12 min., purity = 95.3%.

***N*^{5}-(2-(4-(2,4-dichlorophenyl)piperazin-1-yl)ethyl)-2-(furan-2-yl)-[1,2,4]triazolo[1,5-*a*][1,3,5] triazine-5,7-diamine (12v).** Eluted with EtOAc/MeOH, 5:1 to afford the title compound as white powder (94 mg, yield: 69%). ^{1}H NMR (400 MHz, DMSO-d_6): 8.40 and 8.16 (2 x s due to dimer formation, 2H, NH_2), 7.86 (s, 1H), 7.52 (d, J = 2.0 Hz, 1H), 7.34 (dd, J = 8.4, 2.0 Hz, 1H), 7.25 (t, J = 5.2 Hz, 1H, NH), 7.15 (d, J = 8.4 Hz, 1H), 7.05 (s, 1H), 6.67 (s, 1H), 3.41 (t, J = 5.2 Hz, 2H), 3.10-2.90 (m, 4H), 2.65-2.51 (m, 6H). ^{13}C NMR (101 MHz, DMSO-d_6): 161.2, 159.2, 155.8, 150.0, 148.1, 146.2, 144.6, 129.6, 128.4, 128.0, 126.9, 122.1, 111.9, 111.6, 56.6, 52.8, 50.8, 38.0. HRMS (ESI) *m/z* [*M*+H]$^+$ calcd for $C_{20}H_{22}Cl_2N_9O^+$: 474.13189, found: 474.13182; HPLC: ret. time = 7.98 min., purity = 97.8%.

***N*^{5}-(2-(4-(2-fluoro-4-methoxyphenyl)piperazin-1-yl)ethyl)-2-(furan-2-yl)-[1,2,4]triazolo[1,5-*a*] [1,3,5]triazine-5,7-diamine (12w).** Eluted with EtOAc/MeOH, 5:1 to afford the title compound as white powder (113 mg, yield: 51%). ^{1}H NMR (400 MHz, DMSO-d_6): 8.43 and 8.19 (2 x s due to dimer formation, 2H, NH_2), 7.87 (s, 1H), 7.34 and 7.25 (2 x t due to dimer formation, J = 5.2 Hz, 1H, NH), 7.05-7.04 (m, 1H), 6.97 (t, J = 9.6 Hz, 1H), 6.80 (dd, J = 14.0, 7.6 Hz, 1H), 6.69-6.67 (m, 2H), 3.70 (s, 3H), 3.44-3.41 (m, 2H), 2.91 (br s, 4H), 2.58-2.50 (m, 6H). ^{13}C NMR (101 MHz, DMSO-d_6): 161.6, 161.2,159.2, 156.8, 156.2, 155.9, 155.1, 155.0, 154.4, 150.7, 150.1, 146.2, 144.7, 133.5, 133.4, 119.9, 111.9, 111.7, 109.4, 103.0, 102.8, 57.1, 56.6, 55.5, 52.9, 50.8, 38.4, 38.0. HRMS (ESI) *m/z* [*M*+H]$^+$ calcd for $C_{21}H_{25}FN_9O_2^+$: 454.2037, found: 454.2105; HPLC: ret. time = 11.98 min., purity = 99.4%.

***N*^{5}-(2-(4-(3,4-difluorophenyl)piperazin-1-yl)ethyl)-2-(furan-2-yl)-[1,2,4]triazolo[1,5-*a*][1,3,5] triazine-5,7-diamine (12x).** Eluted with EtOAc to afford the title compound as white powder (14 mg, yield: 25%). ^{1}H NMR (400 MHz, MeOD): δ 7.69 (dd, J = 1.6, 0.8 Hz, 1H), 7.12 (d, J = 3.2 Hz, 1H), 7.06-7.04 (m, 1H), 6.94-6.84 (m, 2H), 6.61 (dd, J = 3.2, 1.6 Hz, 1H), 3.62-3.60 (m, 2H), 3.08-3.07 (m, 4H), 2.75-2.69 (m, 6H). HRMS (ESI) *m/z* [*M*+H]$^+$ calcd for $C_{20}H_{22}F_2N_9O^+$: 442.1837 found: 442.1907; HPLC: ret. time =12.18 min., purity = 95.9%.

Pharmacological characterization

Materials: [^{3}H]-ZM241385 (specific activity 50 Ci mmol^{-1}) was purchased from ARC Inc. (St. Louis, USA). [^{3}H]-1,3-dipropyl-8-cyclopentyl-xanthine ([^{3}H]-DPCPX, specific activity 116.7 Ci/mmol) was purchased from ARC Inc. (St. Louis, USA). Unlabeled ZM241385 was a gift from Dr. S. M. Poucher (Astra-Zeneca, Macclesfield, UK). CGS21680 was a gift from Dr. R. A. Lovell (Ciba-Geigy, Summit, NJ). NECA (5'-*N*-Ethylcarboxamidoadenosine) and DPCPX were purchased from Sigma-Aldrich (Steinheim, Germany). Adenosine deaminase (ADA) was purchased from Boehringer Mannheim (Mannheim, Germany). Bicinchoninic acid (BCA) and BCA protein assay reagent were obtained from Pierce Chemical Company (Rockford, IL, U.S.A.). Human embryonic kidney 293 cells stably expressing the $hA_{2A}R$ (HEK293$hA_{2A}R$) were kindly provided by Dr. J Wang (Biogen/IDEC, Cambridge, MA). Chinese hamster ovary cells stably expressing the hA_1R (CHOhA_1R) were kindly provided by Prof. Steve Hill (University of Nottingham, UK). All other chemicals were of analytical grade and obtained from standard commercial sources.

Cell culture and membrane preparation: Cell culture and membrane preparation were performed as reported previously.[34,43]

Radioligand displacement assay: The radioligand displacement from the hA_1R and $hA_{2A}R$ was determined using the displacement assay as described previously.[34,43]

Radioligand competition association assay: The binding kinetics of unlabeled $A_{2A}R$ ligands were determined at 4 °C using the competition association assay as described previously.[34,43]

cAMP assay: HEK293$hA_{2A}R$ cells were cultured as a monolayer on 10 cm ø culture plates to 80 %-90 % confluency. Cells were harvested and centrifuged two times at 200 × g for 5 min. The amount of cAMP produced was determined with the LANCE® ultra cAMP 384 kit (Perkin-Elmer, Groningen, Netherlands). In general, 1000 cells/well were seeded on 384-well plates and incubated at ambient room temperature (22–25 °C). cAMP generation was performed in the stimulation buffer [*N*-2-hydroxyethylpiperazine-*N*'-

ethanesulphonic acid (HEPES), 5 mM; 0.1 % (w·v^{-1}) BSA; cilostamide, 50 μM; rolipram, 50 μM; adenosine deaminase (ADA), 0.8 IU/mL] Concentration-effect curves for **12x** and **12c** were obtained by adding HEK293hA_{2A}R cells to the mixture of antagonist (**12x** or **12c**) and 100 nM NECA (prepared in the stimulation buffer) for a co-incubation of 30 min. For assessment of either surmountable or insurmountable behavior, the antagonists (**12x** and **12c**) were pre-incubated for 30 min or co-incubated with the agonist NECA at a concentration ranging from 100 μM to 0.1 nM for a duration of 30 min, where the antagonists' concentrations were 0.3-, 1-, 3- and 10-fold their respective K_i values. The incubation was stopped by adding detection mix and antibody solution, according to the instructions of the manufacturer. The generated fluorescence intensity was quantified on the EnVision® Multilabel Reader (PerkinElmer, Groningen, Netherlands). The data obtained were normalized according to the maximal response produced by 100 μM NECA. The shift in agonist EC_{50} was determined to perform Schild analyses.

Data analysis. All experimental data was analyzed by using GraphPad Prism 5.0 (GraphPad Software Inc., San Diego, CA). K_D and B_{max} values of [^{3}H]-ZM241385 at hA_{2A}R membranes were obtained from Guo *et al.*[34] IC_{50} values obtained from competition displacement binding data were converted into K_i values using the Cheng-Prusoff equation.[44] Association and dissociation rates for unlabeled ligands were calculated by fitting the data in the competition association model using '*kinetics of competitive binding*'[30], as described in Chapter 3.

Molecular property descriptors (MW, LogP, MSA, *p*K_a) of the substituted C_2-phenylpiperazine were calculated using MarinSketch 5.11 (ChemAxon, Huagary). (Multiple) Linear regression analysis was done by using Microsoft Excel 2003.

References:

1. Swinney DC. Biochemical mechanisms of drug action: what does it take for success? *Nat Rev Drug Discov* 2004;3(9):801-808.
2. Swinney DC. Can binding kinetics translate to a clinically differentiated drug? From theory to practice. *Lett Drug Des Discov* 2006;3(8):569-574.
3. Nunez S, Venhorst J, Kruse CG. Target-drug interactions: first principles and their application to

drug discovery. *Drug Discov Today* 2012;17(1-2):10-22.
4. Zhang R, Monsma F. Binding kinetics and mechanism of action: toward the discovery and development of better and best in class drugs. Expert Opin Drug Discov 2010;5(11):1023-1029.
5. Copeland RA, Pompliano DL, Meek TD. Drug-target residence time and its implications for lead optimization. *Nat Rev Drug Discov* 2006;5(9):730-739.
6. Rosethorne EM, Turner RJ, Fairhurst RA, Charlton SJ. Efficacy is a contributing factor to the clinical onset of bronchodilation of inhaled beta(2)-adrenoceptor agonists. *Naunyn Schmiedebergs Arch Pharmacol* 2010;382(3):255-263.
7. Govern CC, Paczosa MK, Chakraborty AK, Huseby ES. Fast on-rates allow short dwell time ligands to activate T cells. *Proc Natl Acad Sci U S A* 2010;107(19):8724-8729.
8. Foote J, Eisen HN. Kinetic and affinity limits on antibodies produced during immune responses. *Proc Natl Acad Sci U S A* 1995;92(5):1254-1256.
9. Schreiber G. Kinetic studies of protein-protein interactions. *Curr Opin Struct Biol* 2002;12(1):41-47.
10. Selzer T, Albeck S, Schreiber G. Rational design of faster associating and tighter binding protein complexes. *Nat Struct Biol* 2000;7(7):537-541.
11. Sykes DA, Dowling MR, Leighton-Davies J, Kent TC, Renard E, Trifilieff A, Charlton SJ. The Influence of Receptor Kinetics on the Onset and Duration of Action, and the Therapeutic Index of NVA237 and Tiotropium. *J Pharmacol Exp Ther* 2012;343(2):520-528.
12. Fredholm BB, IJzerman AP, Jacobson KA, Linden J, Müller CE. International Union of Basic and Clinical Pharmacology. LXXXI. Nomenclature and classification of adenosine receptors--an update. *Pharmacol Rev* 2011;63(1):1-34.
13. Jacobson KA, Gao ZG. Adenosine receptors as therapeutic targets. *Nat Rev Drug Discov* 2006;5(3):247-264.
14. Shook BC, Jackson PF. Adenosine A_{2A} Receptor Antagonists and Parkinson's Disease. *ACS Chem Neurosci* 2011;2(10):555-567.
15. Muller CE, Jacobson KA. Recent developments in adenosine receptor ligands and their potential as novel drugs. *Bba-Biomembranes* 2011;1808(5):1290-1308.
16. Shah U, Hodgson R. Recent progress in the discovery of adenosine A_{2A} receptor antagonists for the treatment of Parkinson's disease. *Curr Opin Drug Discov Devel* 2010;13(4):466-480.
17. Poucher SM, Keddie JR, Singh P, Stoggall SM, Caulkett PW, Jones G, Coll MG. The *in vitro* pharmacology of ZM 241385, a potent, non-xanthine A_{2a} selective adenosine receptor antagonist. *Br J Pharmacol* 1995;115(6):1096-1102.
18. Caulkett PWR, Jones G, Collis MG, Poucher SM; Imperial Chemical Indusry PLC, London, assignee. UK. 1991.
19. Vu CB, Pan D, Peng B, Kumaravel G, Smits G, Jin X, Phadke D, Engber T, Huang C, Reilly J, Tam S, Grant D, Hetu G, Petter RC. Novel diamino derivatives of [1,2,4]triazolo[1,5-*a*][1,3,5]triazine as potent and selective adenosine A_{2a} receptor antagonists. *J Med Chem* 2005;48(6):2009-2018.
20. Vu CB, Peng B, Kumaravel G, Smits G, Jin X, Phadke D, Engber T, Huang C, Reilly J, Tam S, Grant D, Hetu G, Chen L, Zhang J, Petter RC. Piperazine derivatives of [1,2,4]triazolo[1,5-*a*][1,3,5]triazine as potent and selective adenosine A_{2a} receptor antagonists. *J Med Chem* 2004;47(17):4291-4299.
21. Vu CB, Shields P, Peng B, Kumaravel G, Jin X, Phadke D, Wang J, Engber T, Ayyub E, Petter RC. Triamino derivatives of triazolotriazine and triazolopyrimidine as adenosine A_{2a} receptor antagonists. *Bioorg Med Chem Lett* 2004;14(19):4835-4838.
22. Dolzhenko AV, Dolzhenko AV, Chui WK. Practical synthesis of regioisomeric 5(7)-amino-

6,7(4,5)-dihydro[1,2,4]triazolo[1,5-*a*][1,3,5]triazines. *Tetrahedron* 2007;63(52):12888-12895.
23. Dolzhenko AV, Pastorin G, Dolzhenko AV, Chui WK. An aqueous medium synthesis and tautomerism study of 3(5)-amino-1,2,4-triazoles. *Tetrahedron Lett* 2009;50(18):2124-2128.
24. Jorg M, Agostino M, Yuriev E, Mak FS, Miller ND, White JM, Scammells PJ, Capuano B. Synthesis, molecular structure, NMR spectroscopic and computational analysis of a selective adenosine A(2A) antagonist, ZM 241385. *Struct Chem* 2013;24(4):1241-1251.
25. Jorg M, Shonberg J, Mak FS, Miller ND, Yuriev E, Scammells PJ, Capuano B. Novel adenosine A(2A) receptor ligands: A synthetic, functional and computational investigation of selected literature adenosine A(2A) receptor antagonists for extending into extracellular space. *Bioorg Med Chem Lett* 2013;23(11):3427-3433.
26. Caulkett PWR, Jones G, McPartlin M, Renshaw ND, Stewart SK, Wright B. Adenine isosteres with bridgehead nitrogen. Part 1. Two independent syntheses of the [1,2,4]triazolo[1,5-*a*][1,3,5] triazine ring system leading to a range of substituents in the 2, 5 and 7 positions. *J Chem Soc, Perkin Trans* 1 1995(7):801-808.
27. Tenbrink RE. Pharmacia & Upjohn Company, MI, assignee. USA. 1999.
28. Martin GE, Elgin RJ, Jr., Mathiasen JR, Davis CB, Kesslick JM, Baldy WJ, Shank RP, DiStefano DL, Fedde CL, Scott MK. Activity of aromatic substituted phenylpiperazines lacking affinity for dopamine binding sites in a preclinical test of antipsychotic efficacy. *J Med Chem* 1989;32(5):1052-1056.
29. Morita S, Kitano K, Matsubara J, Ohtani T, Kawano Y, Otsubo K, Uchida M. Practical application of the palladium-catalyzed amination in phenylpiperazine synthesis: An efficient synthesis of a metabolite of the antipsychotic agent aripiprazole. *Tetrahedron* 1998;54(19):4811-4818.
30. Motulsky HJ, Mahan LC. The kinetics of competitive radioligand binding predicted by the law of mass action. *Mol Pharmacol* 1984;25(1):1-9.
31. Vauquelin G, Van Liefde I, Vanderheyden P. Models and methods for studying insurmountable antagonism. *Trends Pharmacol Sci* 2002;23(11):514-518.
32. Kenakin T, Jenkinson S, Watson C. Determining the Potency and Molecular Mechanism of Action of Insurmountable Antagonists. *J Pharmacol Exp Ther* 2006;319(2):710-723.
33. Vauquelin G, Szczuka A. Kinetic versus allosteric mechanisms to explain insurmountable antagonism and delayed ligand dissociation. *Neurochem Int* 2007;51(5):254-260.
34. Guo D, Mulder-Krieger T, IJzerman AP, Heitman LH. Functional efficacy of adenosine A_{2A} receptor agonists is positively correlated to their receptor residence time. *Br J Pharmacol* 2012;166(6):1846-1859.
35. Sykes DA, Dowling MR, Charlton SJ. Exploring the mechanism of agonist efficacy: a relationship between efficacy and agonist dissociation rate at the muscarinic M_3 receptor. *Mol Pharmacol* 2009;76(3):543-551.
36. Mantell SJ, Stephenson PT, Monaghan SM, Maw GN, Trevethick MA, Yeadon M, Keir RF, Walker DK, Jones RM, Selby MD, Batchelor DV, Rozze S, Chavaroche H, Hobson TJ, Dodd PG, Lemaitre A, Wright KN, Stuart EF. Inhaled adenosine A(2A) receptor agonists for the treatment of chronic obstructive pulmonary disease. *Bioorg Med Chem Lett* 2008;18(4):1284-1287.
37. Andersson K, Karlsson R, Lofas S, Franklin G, Hamalainen MD. Label-free kinetic binding data as a decisive element in drug discovery. *Expert Opin Drug Dis* 2006;1(5):439-446.
38. Gabrielsson J, Dolgos H, Gillberg PG, Bredberg U, Benthem B, Duker G. Early integration of pharmacokinetic and dynamic reasoning is essential for optimal development of lead compounds: strategic considerations. *Drug Discov Today* 2009;14(7-8):358-372.
39. Liu W, Chun E, Thompson AA, Chubukov P, Xu F, Katritch V, Han GW, Roth CB, Heitman LH,

IJzerman AP, Cherezov V, Stevens RC. Structural basis for allosteric regulation of GPCRs by sodium ions. *Science* 2012;337(6091):232-236.

40. Xu F, Wu H, Katritch V, Han GW, Jacobson KA, Gao ZG, Cherezov V, Stevens RC. Structure of an agonist-bound human A_{2A} adenosine receptor. *Science* 2011;332(6027):322-327.
41. Dror RO, Pan AC, Arlow DH, Borhani DW, Maragakis P, Shan Y, Xu H, Shaw DE. Pathway and mechanism of drug binding to G-protein-coupled receptors. *Proc Natl Acad Sci U S A* 2011;108(32):13118-13123.
42. Kruse AC, Hu J, Pan AC, Arlow DH, Rosenbaum DM, Rosemond E, Green HF, Liu T, Chae PS, Dror RO, Shaw DE, Weis WI, Wess J, Kobilka BK. Structure and dynamics of the M3 muscarinic acetylcholine receptor. *Nature* 2012;482(7386):552-556.
43. Guo D, van Dorp EJ, Mulder-Krieger T, van Veldhoven JP, Brussee J, IJzerman AP, Heitman LH. Dual-point competition association assay: a fast and high-throughput kinetic screening method for assessing ligand-receptor binding kinetics. *J Biomol Screen* 2013;18(3):309-320.
44. Cheng Y, Prusoff WH. Relationship between the inhibition constant (K_I) and the concentration of inhibitor which causes 50 per cent inhibition (I_{50}) of an enzymatic reaction. *Biochem Pharmacol* 1973;22(23):3099-3108.